AUTHORS

KAI PACHECO:
Using Cellular Automata to Treat Cardiac Arrhythmias
GEORGE DRIMBA:
Categorizing Point Sets with No Empty Pentagons

NOTICE TO AUTHORS

MATH SURVEY is the annual student journal of the Stuyvesant High School Mathematics Department. Students are invited to submit papers written during research courses or programs, as well as synopses of subjects learned in school or in private study. Written material need not represent original theory, but may instead summarize or explain a subject. Appropriate subjects include all aspects of mathematics and computer science not encountered in the standard high school curriculum. Papers written during the freshman year must be accompanied by a brief recommendation from the directing researcher or faculty member.

Each paper submitted to MATH SURVEY will be read by a faculty referee, who will convey notice through the editor of whether the paper has been accepted, and if so, what improvements are to be required; these may be mathematical or stylistic. The editorial staff reserves the right to alter final submitted drafts in point of style, wording, and layout.

Our readers expect to a high level of both scholarship and exposition. To be a good candidate, an article should first contain important and challenging mathematical ideas. The writing should be clear and straightforward, so that the content may speak for itself. Sufficient background should be given so that a non-expert may learn and profit from each article.

Authors should submit their work in the LaTeX markup language if possible. Other submissions will be rendered in LaTeX at the discretion of the editors. To learn our formatting style, as well as how to properly cite other published materials, please examine the present volume. All submissions should be sent to the Faculty Advisor.

Contents

1 Editor's Notes **3**

2 Foreword **4**

3 Using Cellular Automaton Automata to Treat Cardiac Arrhythmias **7**

4 Categorizing Point Sets with No Empty Pentagons **27**

5 Proofs Without Words **34**

6 Problems **36**

7 Solutions **38**

1 Editor's Notes

Dear Reader,

The year is 1927. The international headlines laud Charles Lindberg's solo non-stop transatlantic flight from New York City to Paris. National headlines proclaim the start of a new granite sculpture of four presidents in Mount Rushmore. New York City headlines announce the opening of the Holland Tunnel. But few take notice of the inaugural edition of the publication you now hold in your hand. Yet, 88 years later, the Math Survey endures as the official publication of the Mathematics Department of Stuyvesant High School.

To what do we owe this exceptional longevity? First, we must acknowledge the intrinsic beauty and timeless relevance of math itself. Well before the dawn of the Math Survey, Galileo considered the profound nature of mathematics:

> *Philosophy is written in this grand book - I mean the universe - which stands continually open to our gaze, but it cannot be understood unless one first learns to comprehend the language in which it is written. It is written in the language of mathematics, and its characters are triangles, circles, and other geometric figures, without which it is humanly impossible to understand a single word of it; without these, one is wandering about in a dark labyrinth.*

Second, we must recognize the generations of students, faculty, and administrators who share a passion for mathematical research, problem solving, and instruction. Math Survey continues to provide an opportunity for Stuyvesant's math community to showcase the best of its students' insights and efforts. I would like to express my gratitude to the people who continue to promote our longstanding mission: the staff, the contributors, Mr. Jumash, Ms. Ferrara, and Ms. Zhang. Thanks to them, the Math Survey illuminates one corner of a dark labyrinth.

As you process the articles, problems, and proofs without words, I hope that you enjoy this ongoing testament to the greatness of mathematics.

Sincerely,

Calvin Lee

Editor

2 Foreword

by Peter Brooks

Peter Brooks has taught mathematics and computer science at Stuyvesant since 2005. He received his Bachelor's degree in mathematics from Caltech, an M.A. in economics from The New School, and an M.A. in Math Education from Teachers College, Columbia. In 1984, he founded MicroMind, Inc., a software development company which he ran for 13 years. Along the way, he co-developed the first interpreter for the C language, and later created one of the first world-wide-web browsers, for which he received a national award. He also created seven other software products for the market. In 2003, he was invited to Stuyvesant to give some talks to students on advanced mathematics and computer science ideas. Soon after that experience, he gave up full-time software development to get his teaching license. The rest is local history.

I'd like to thank everyone involved for all the work of creation; for the long hours spent on finding and refining ideas, then searching for the words to express them and smoothing the flow of exposition. And, of course, thanks to all for the work of production: for choosing, copy-editing, transcription, layout. And to the editors and particularly Aziz Jumash, without whose nudging this forward would have ended approximately here.

I have been thinking about the pleasures of mathematics - pleasures public and private, from high to distinctly low. I remember some of them from when I was a student, and would like, now, to distinguish them from each other, and from the current ones I have as a teacher.

High pleasure is easy, books are dedicated to it. We share company with grand mathematical thoughts; universes are captured in a minimum of symbols. For instance, Euclid's proof of the infinitude of primes in two sentences implies that there is a vast storehouse out there, but does so with a minimalist elegance in showing but a single occupant of it. Neat. Euler's equation, $e^{i\pi} + 1 = 0$, which graced my wall for decades, implies the existence of mysterious tunnels between arithmetic, algebra, geometry and calculus, and so gave me a glimpse of some monstrously grand order beneath the jumble of high school math topics. The Generalized Stokes Theorem ...

$$\int_{\partial\Omega} \omega = \int_{\Omega} d\omega$$

. . . if you know what the symbols mean, contains the Fundamental Theorem of Calculus and Green's Theorem and the Divergence Theorem, and can live on reasonable manifolds in all dimensions - this pulls you above the clouds to show off a vast domain. These are the big gems, but then there are also mini-gems and micro-gems, enough to keep you going on the bad days when the problems don't work out and the pieces don't quite connect. These are the joys of the apprehension of Beauty and the power over ideas.

But let's step down a bit. Let's say that I've just solved a hard math problem, with what I consider to be a very elegant solution. Why do I feel so good? Well . . . I've successfully accomplished a difficult task, with the bonus of elegance. And because it was difficult, few others could do it, and that feeds my self-esteem - the human ego is a needy taskmaster, and will shortly suggest more of the same. This, I submit, is what gets many of us going, early on - not simply being good at arithmetic, but better than. Math is a particularly nice safe haven for the teen years, praised by adults, unlike, say, talents in machine shop or drums (though not as sexy amongst peers). And it's a gift that keeps on giving, for the rewards to mathematical proficiency don't expire quickly. There's nothing wrong with this - it's just the muck of ordinary life - the substructure that supports the weight and effort of the higher enterprise. And thank goodness for it, since few of us can sustain ourselves entirely on a diet of rarified thoughts.

But it's not all ego. We have to talk about flow, that feeling of rightness and competence when we're firing on all cylinders and coming in under time and budget. It is that sense of mastery that allows us to see connections between the problems we're solving and the parent ideas, and their relations and more distant relatives. It is when our intuition has pulled just the right tools from our math shopping bag and they fit snugly and do the job.

However, let me mention another source of joy, closer to my home: teaching. We claim respect from satisfying students' need to know, though occasionally it's our need to tell. The more arrogant of us might say that if you haven't told a really good joke or proven a really cool theorem, you haven't lived - actually, there's a lot of similarity between those two. A teacher will be tempted to structure a proof so that you don't see the crucial piece coming until just before the end, same as a comic - while this is not good pedagogy, it is the pleasure of showmanship. But this is not the driver. The driver is the occasional, and if we're very lucky, the frequent understandings of the

grand patterns we can pull out of our pockets. The connections, analogies, mappings, groups – all of the moments of "let me show you this" - that's the driver. And you sense, on the good days, on the home run days, that it's a bit unfair to be paid for this on top of it all. And then we send the students off, four years older and a foot taller, with a packed toolbox to play with patterns. And turn around and see a new, shorter group.

I recommend this.

Sincerely,

Peter Brooks

3 Using Cellular Automaton Automata to Treat Cardiac Arrhythmias

by Kai Pacheco

Abstract

Cardiac rotors, spiral waves, and bad nodes cause many of the most devastating heart conditions. Unfortunately, not enough is known about these perturbations to always completely fix them and stop them from recurring in the future. This is due to the fact that it is extremely difficult to detect where these reentrant circuits originate. A novel cellular automaton simulation of the cells in the heart tissue models how these rotors and spirals develop as a result of a specific group of sick cells which, if eliminated, would solve the issue indefinitely. A subset of signals, simulating an array of real electrode recordings, is extracted and fed into another program. From this electrode data, Barycentric Interpolation is used to approximate the behaviors of the cells in between the electrodes, in order to estimate the original disrupted wave. An algorithm can then be developed to identify and target the faulty cells.

Introduction and Fundamental Notions

The heart beats more than 2.5 billion times over an average lifetime. Every single one of these pulses has the potential to err somewhere and cause a reentrant circuit. That is why it is essential to understand the mechanisms of cardiac arrhythmias caused by faulty cells, rotors or spiral waves in the electrical propagating waves in the heart. We can focus down to the cellular level to replicate and fix issues that cause irregular or rapid heartbeats, otherwise known as Cardiac Arrhythmias.

What Are Rotors and Spiral Waves?

Problems in the electrophysiology of the heart typically occur because of the electrical interaction of adjacent cells. To understand these cells' behavior we must first understand the concept of depolarization. Depolarization occurs when a cell's membrane potential drastically changes from a negative charge to a positive charge, or becomes active. Furthermore, cells are triggered to depolarize when their neighboring cells depolarize; so in concept, a large chain reaction of depolarization can occur in response to a single cell's depolarization. Ideally, this consequential wave spreads throughout the cells and the four chambers, starting with a single cell's depolarization. This starting point is located at a self-triggering cell called a node. The main node that sets the pace of the electrical

waves is known as the Sinoatrial (SA) Node. Action potentials originate at this node and travel through the heart, assisted by fast acting strips known as bundles (tracts). Sometimes, however, at a certain point in a cycle, the wave can turn around due to faulty cells, causing a bad cycle of waves to propagate in the wrong direction. These reentrant circuits are due to faulty cells and sometimes form rotors or spiral waves. Although many use the terms "rotor" and "spiral wave" interchangeably, because they both cause these reentrant circuits, they have distinguishable differences in structure and development. Although both make spiral-like patterns, rotors occur when depolarization waves loop around a group of dead cells, faulty cells, or holes (structures like the Pulmonary Veins), while spiral waves spiral around an electrically hollow point (like a pinwheel).

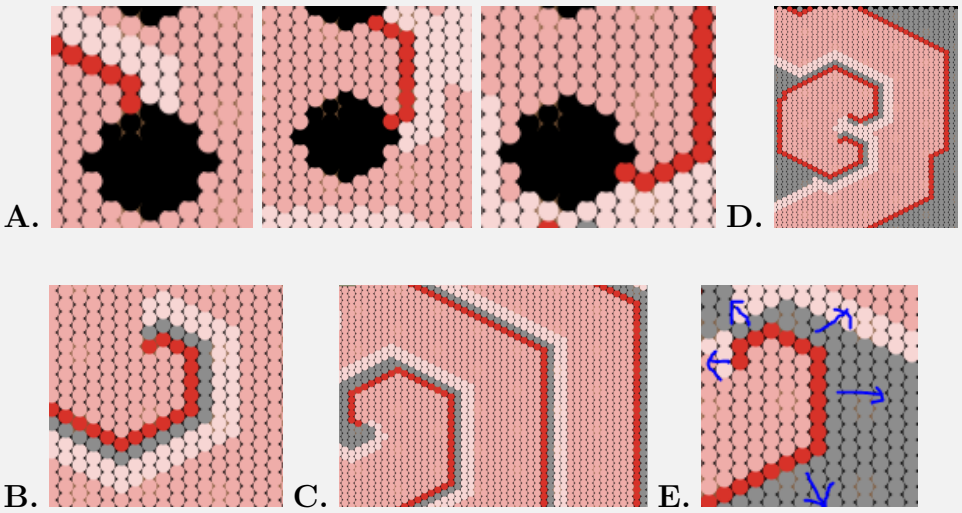

Rotors and Spirals

A. A rotor causes a wave to progress around a pulmonary vein

B. A spiral wave circles around indefinitely in a patch of otherwise healthy cells.

C. A spiral wave can create multiple, rapid pulses that eventually take over the SA node due to its faster pace.

D. Oftentimes a double spiral wave forms looping in from either side.

E. The energy of the waves produced by rotors and spiral waves are directed outward.

Refer to **Figure 1A** to view a simulated rotor and **Figure 1B** to view a simulated Spiral Wave. When a reentrant circuit occurs without forming a rotor or spiral, it is due to a faulty cell directly impacting the circuit by starting its own unwanted wave. One common type of faulty cell is one with an unreasonably short cycle time. This creates another starting point that takes over the heartbeat in that region, moving the wave in the wrong direction and causing ineffective pumping. Since it behaves like a node where it is not supposed to, we call this a bad node.

Overall, there are three mechanisms addressed here that make the heart beat irregularly: rotors, spiral waves, and bad nodes. These are what typically cause problems like atrial fibrillation, bradycardia, and atrial flutter.

The Electrophysiological Behavior of Cells

To continue, we must focus further into the cellular level. With the exception of nodes, each cell goes through five phases in its depolarization cycle. These phases can be seen below in **Figure 2**.

Cell Voltage vs. Time

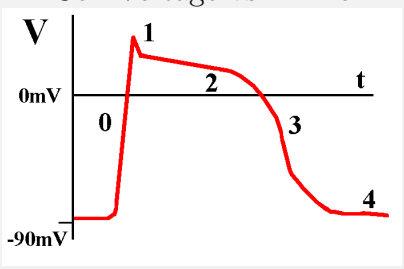

0 = Rise Phase (about 20 milliseconds)

1 = Peak Phase (instantaneous)

2 = Hold Phase (about 120 milliseconds)

3 = Fall Phase (about 60 milliseconds)

4 = Rest Phase (about 2000 milliseconds)

*The dashed line is the peak threshold

In the cell's Rest Phase (4), the cell's voltage (or potential) is very low. Referred to as unexcited, the cell is still at a highly negative potential (generally around -80 to -90 Millivolts) waiting to be depolarized or activated. Next, when triggered to depolarize, the cell goes through its Rise Phase (0). In this stage, the cell voltage quickly rises from a negative to a positive voltage, depolarizing. The next and shortest, almost instantaneous stage is the Peak Phase (1). During this phase, the voltage of the cell reaches its peak and immediately drops off slightly. When the cell voltage plateaus at a positive voltage after returning from its peak, it is in its Hold Phase (2). As the voltage slowly begins to drop again to its negative origin, the cell is in its Fall Phase (3). Less rapidly than the rise phase, the cell's voltage drops back to its highly negative Rest Phase. There are two important thresholds to note here: The 0mV threshold and the peak threshold. Only below the 0mV threshold is the cell vulnerable to being triggered by others and only above the peak threshold is the cell able to trigger others. This means that the cell is resistant to retriggering during its entire Hold Phase and some of its Rise and Fall Phases. In addition, it can only induce retriggering in its neighboring

cells when it is at its Peak Phase.

Cells also have an emergency mechanism, in case they are not triggered for a long time. If a normal cell is left in its rest phase for too long a time without being retriggered, it eventually reaches a threshold where it retriggers on its own.

What causes cells to be categorized as faulty or "sick" is an irregularity of the time in one or more of its phases. Factors ranging from lack of nutrients (such as sodium and oxygen) to injuries in the cell can cause these phase times to become longer or shorter than those of a healthy cell, thereby disrupting the uniformity of activation of the cells in the heart. This in turn could cause the cell interactions to become disorganized, thus creating re-entrant circuits of depolarization.

How Rotors, Spirals, and Bad Nodes Create Reentrant Circuits

Most of the time, slightly sick cells do not affect the regularity of the pace of the waves. This is because the immunity mechanism of cells in the middle of their depolarization protects them from faulty retriggers, as seen in **Figure 3B**. However, sometimes sick cells are so defective that their dynamic configurations can disrupt the normal wave pattern. As noted earlier, these disruptions are caused by three distinguishable mechanisms: rotors, spiral waves, and faulty cells.

Figure 3. The Behavior of Depolarization Waves around Dead Cells

A. As seen from left to right, the frames of the animation show how a wave of even an oddly shaped area of dead cells will always meet its other end when moving in the same direction.

B. A group of sick cells are trapped in the wave and cause no harm to the flow of the pulse.

To understand what cause rotors and spiral waves to develop, it is important to note what doesn't. Completely dead cells are cells that will never trigger others nor be triggered by others. Although dead cells may aid in creating reentrant circuits, they are never alone the cause of these.

Refer to **Figure 3A** to understand why this is the case. Instead, the existence of faulty living cells, or sick cells, initiate the bad patterns of arrhythmias.

Since each cycle around a spiral creates a wave outwards (as seen in **Figure 1C**), the smaller the rotor or spiral, the more devastating, in that it makes more rapid irregular pulses and are more difficult to locate. Sometimes some of the worst cases of arrhythmia are also the hardest to detect and fix or even simply improve.

Current Therapies for Arrhythmias

The only way to fix many rotors is through a process called Ablation, in which a doctor kills an area of tissue in the heart, not necessarily to kill the sick cells themselves, but to trap or isolate the bad wave.

Ideally, targeting and killing the few bad cells that actually cause the issue would bring the heart back to normal again without a possibility of reoccurrence. Unfortunately, because it is so difficult for doctors to detect the specific locations of where the bad cells are, inaccurate methods are used. Therefore, it is a huge challenge to fix rotors. Even if they do temporarily fix it, there is currently no way of knowing whether or not the problem is actually solved. This is because current methods are limited to learning from trial and error. For example, one common attempt to fix rotors around the left pulmonary veins is to use *Pulmonary Vein Isolation*, in which doctors kill cells in a circular pattern around each vein, left and right, inferior (upper) and superior (lower) or set of veins (inferior and superior) where the arrhythmia is often coming from. However, besides the fact that this method is only successful part of the time, it is extremely inefficient, as the problem is many times occurring as a result of only a small group of bad cells that could just be eliminated directly to solve the problem. Instead, Pulmonary Vein Isolation kills and blocks off big chunks of cells around the veins.

Other ablations are similarly far from perfect. Currently, doctors also use the *Cox-Maze* method to guide where to ablate in an irregular beating heart, seen in **Figure 4**. Using the Cox Maze approach, doctors make incisions or ablate in a maze-like pattern to attempt to disrupt the bad waves of depolarization and guide the good waves, which are those initiated by the SA Node, into the maze pattern. However, much like Pulmonary Vein Isolation, this method is far from efficient, killing and blocking many more cells in the heart than necessary. It kills and blocks an even bigger chunk of cells than Pulmonary Vein Isolation. Also, even the best ablation practitioners are only successful less than 90 percent of the time and patients' normal rhythms are oftentimes adversely

affected after the procedure, because the electrical waves have to propagate around the long lines of affected tissue.

Figure 4. Cox Maze Procedure for Atrial Fibrillation

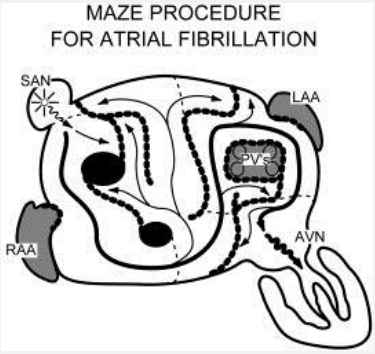

Doctors cut the atriums up into this maze-like pattern in order to direct the healthy wave in one specific path.

The Simulation of the Electrical Heart

Using Netlogo, an agent-based programming language and integrated modeling environment, we can create a cellular automaton that simulates the activation wave that spreads across the left atrium at a macro cellular level, starting from the entry point on a bundle known as the Bachmann's Bundle. It illustrates the electrical wave across the atrium by simulating the behavior of cells and their interaction with each other in a real time animation. **Figure 5** shows the animation's basic setup.

The reason why the left atrium was chosen for this simulation is that many of the arrhythmias and recurring issues in the electrical system of the heart occur there. Also, many of the problems that occur here are representative of problems that occur electrically in any other part of the heart. The program shows the front of the left atrium in the lower half and the rear, as if it were flipped up and over the front, in the upper half.

Figure 5. Simulation of the Left Atrium

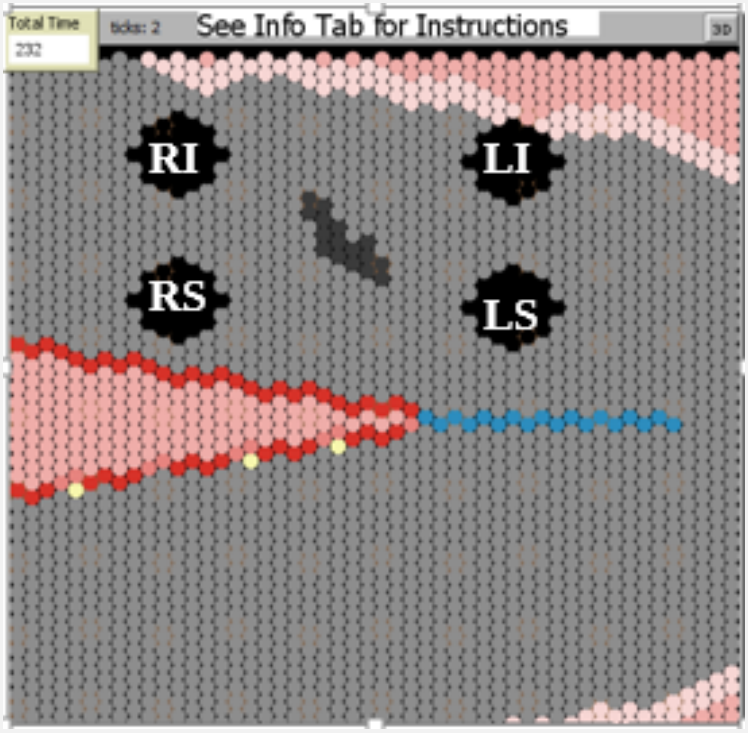

RI = Right Inferior Pulmonary Vein

RS = Right Superior Pulmonary Vein

LI = Left Inferior Pulmonary Vein

LS = Left Superior Pulmonary Vein

Color Key:

Gray: A cell that it is in its Rest Phase.

White: A cell that has just been triggered

Red: A cell that is in its Rise Phase

Pink: A cell that is in its Hold Phase

Light Pink: A cell that is in its Fall Phase

Dark Gray: A dead cell

Black cells: A hole (no cells exist there)

Blue: cells that are part of the Bachmann's Bundle

This particular program simulates the mechanics behind the development of rotors and spirals as well as simulate the real life methodology behind performing therapeutic tasks like cardioversions,

ablations, and pulmonary vein isolation to fix these rotors and spirals. Thus, the user of the program has the ability to select individual or groups of cells and change their properties, such as rest, hold, rise, and fall times, or set them to be dead cells, bundle cells, holes, or normal cells (essentially erasing cells previously set to anything not normal). Green cells are those currently selected by the user for the purpose of manually changing their properties. See **Figure 6**.

Every cell in the program is its own object and has the following several properties that are measured not in pure time, but in number of ticks. The normal, healthy cell's uninterrupted Rest Time lasts 600 ticks before it would retrigger on its own, while Rise Time lasts 6 ticks, Hold Time lasts 60 ticks, and Fall Time lasts 12 ticks. I've made the ratio of the ticks between each of the phases similar to that of real heart tissue cells. At every tick, each cell has its own values for phase times and either being dead, a hole, a bundle, or a bad. Thus, there could be various configurations of cells that can cause different results.

Figure 6. Draw Function

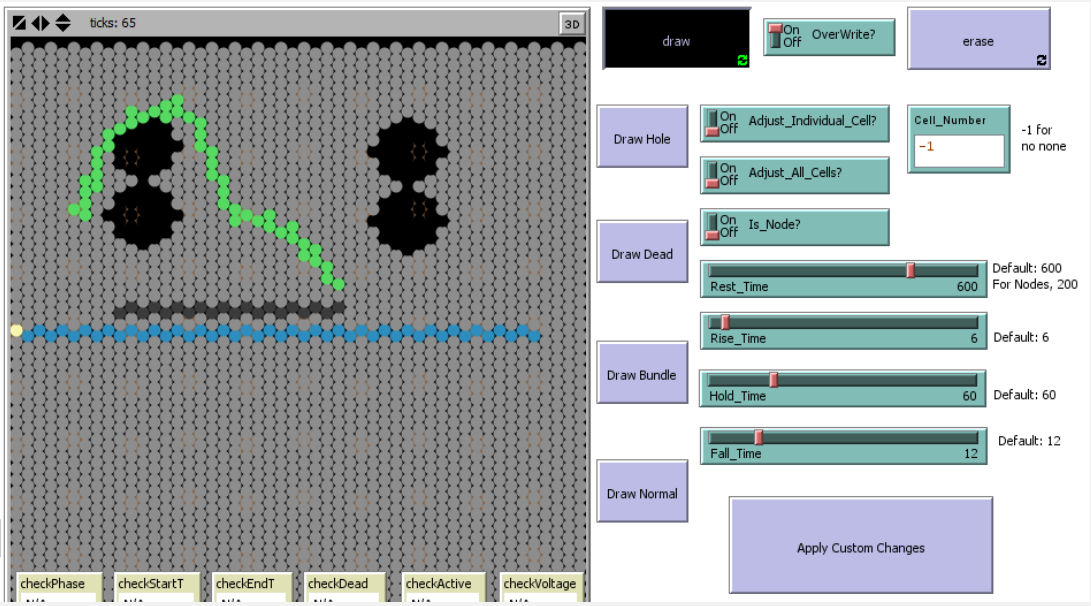

The user in this figure is in the midst of selecting a group of cells to change, by adjusting the knobs above.

There are several default configurations available for loading that simulate the realistic setup of Bachmann's Bundle and the pulmonary veins. Additionally, different levels of randomness can be applied at every tick allow for a more realistic simulation of cellular activity. **Figure 7** shows some of these levels.

Figure 7. Levels of Randomness

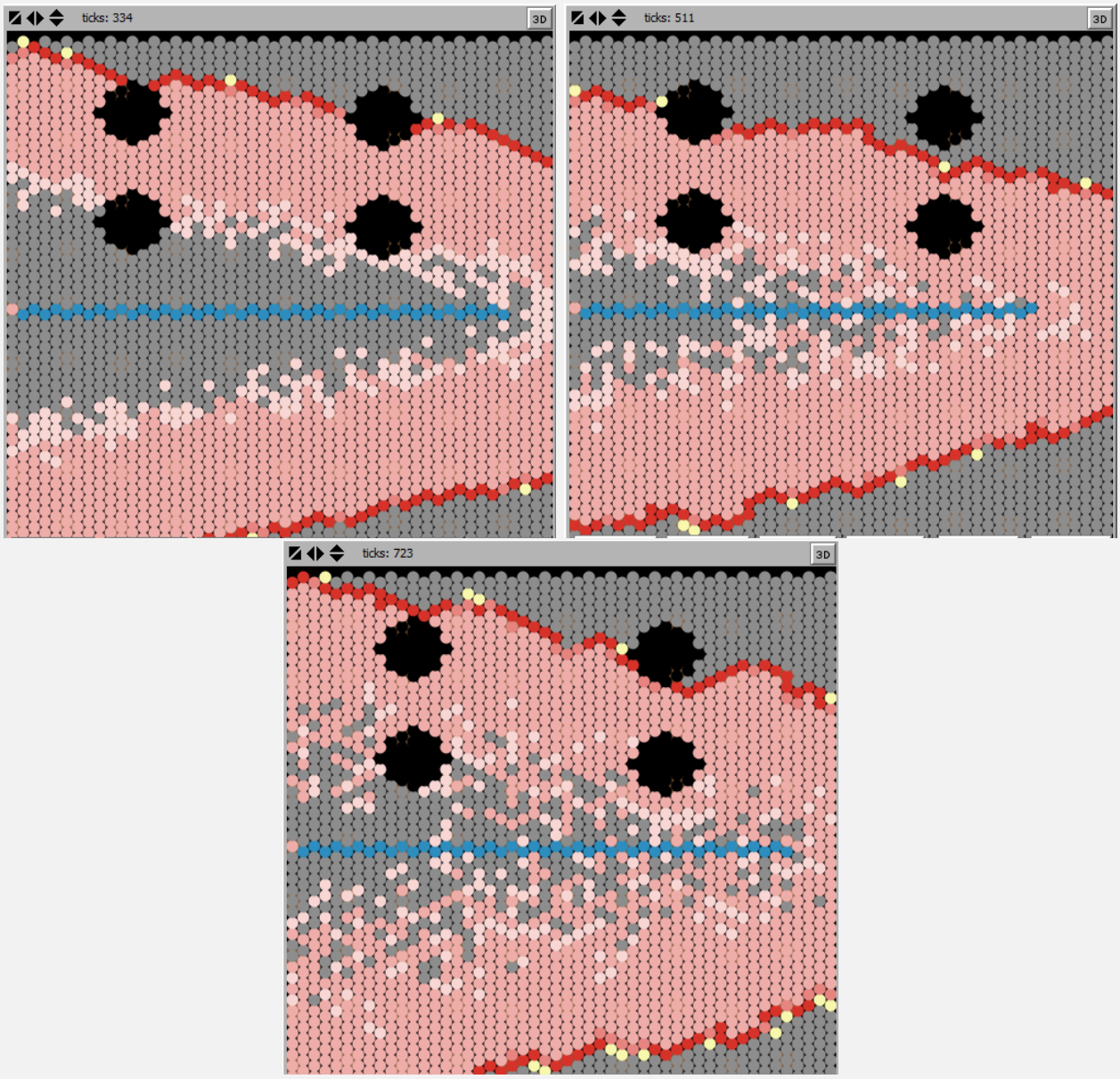

The randomness can be altered throughout the animated simulation. This is done by randomly changing the phase times by a certain ratio. This randomness can be held constant or it can be changed ever pulse.

There are also configurations representing common structural defects. Additionally, multiple configuration files can be loaded on top of each other. Since the configuration files are a list of altered (non-normal) cells, this allows for the user to create a configuration that simulates the development of a problem and load on top of that another configuration that attempts to solve that problem. Other features which help with understanding, usability, realism, and application to real

life medical technologies are shown in **Figure 8**.

Figure 8. Rotors and Spirals

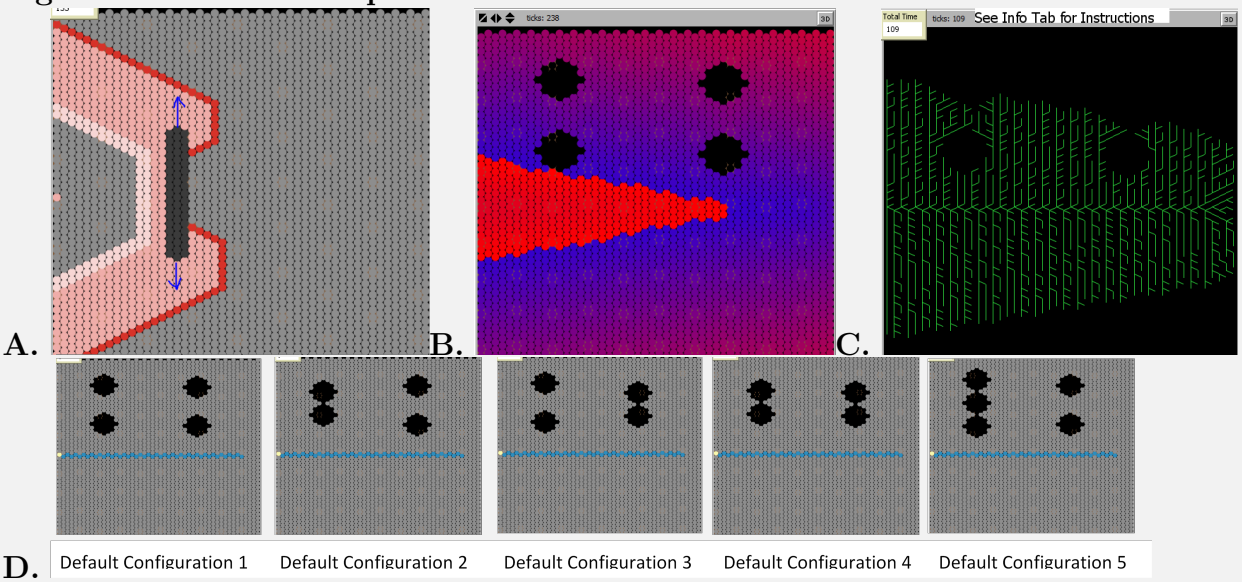

A. The Vortex Shedding feature creates spiral waves or double spiral waves through vortex shedding. Vortex Shedding is a phenomenon where an oscillating body disrupts the flow of a wave.

B. The Color Map feature allows the user to view the animated wave flow with Color Flow Imaging. Red cells are cells that have just been activated while blue cells are cells that have last been activated.

C. The Skeleton feature allows the user to view the individual path of the wave at each cell. Each branch should trace back to the node it came from.

D. Several types of default configurations of cells can be loaded up. Each represent different types of realistic Pulmonary Vein arrangements generally occur in the left atrium.

The Simulation of Rotors, Spiral Waves, and Bad Nodes

After experimenting with a lot of different static and dynamic configurations (where the cell properties change mid-animation), I was successful in simulating the development of spirals and rotors that could be reproduced with specific saved configurations of cells.

Using this animated view of the electrophysiology in the left atrium, based on the behaviors of individual cells interacting with each other, the development of rotors and spirals are easily visualized. Spirals or ongoing rotors could not simply be formed through a static configuration of cells, but an occasional rotor could. Occasional rotors cause irregular heartbeats that develop a bad loop in the 2nd or 3rd pulse. On the other hand, rotors and spiral waves that continue to loop

around indefinitely can only be caused dynamically changing the phase times in the middle of the animation.

Realistically, the spirals and continuing rotors are the causes of very sudden fibrillation attacks that seem spontaneous when they happen, while occasional rotors cause long-term heartbeat problems. Seemingly healthy cells that briefly and drastically change would be likely to cause multiple devastating spirals. It is the pure act of this sudden change or transition that actually causes the spirals, not the simple fact that it is sick. Some spirals and rotors were able to be created by vortex shedding or just by having briefly sick cells that become better in the middle of the animation. **Figure 8A** shows how Vortex Shedding produces these spirals.

The rotors formed from setting a stagnant configuration of cells, however, simulate reoccurring problems because there is no change. These are the types of issues doctors struggle with most today. In the end, whether it is a group of cells that causes consistent rotors every other beat, or a group of cells that keep becoming sick and causing sudden fibrillation attacks, the only way to stop the problem is to kill or trap the bad cells that keep causing this.

The Simulation of Real Therapies to Treat Artificial Arrhythmias

Cardioversion worked successfully in immediately fixing all continuing spirals or rotors that were caused by sudden change. Cardioversion was simulated by simultaneously setting each cell to the beginning of its Rise Phase. However, many times the cells that were changing to cause the spiral in the first place do the same thing later and the same problem reoccurs in the future. Thus, cardioversion would be only a temporary fix. The only way to fix the reoccurring problem is to get rid of the sick cell. The simulation also succeeds in imitating ablations that are only successful when performed in the right place. Finally, killing every altered cell from a loaded configuration successfully fixed any arrhythmia at any time in the simulation.

Artificial Signal Processing to Detect Arrhythmias

Since the simulation is able to save configurations of cells that develop rotors and fix them, it is possible to simulate how doctors could figure out where the problem is and how to treat it based on measured voltages and activation times. In other words, it is important to simulate real world data by acquiring information of a rotor strictly based on its activation pulses and times, rather than through the interactions of individual cells and their behavior. Thus, another feature of the simulation allows the user to save within an Activations file, multiple cycles' worth of only cells'

activation times relative to each other.

Figure 9. The Cellular and Electrode Signal Processor

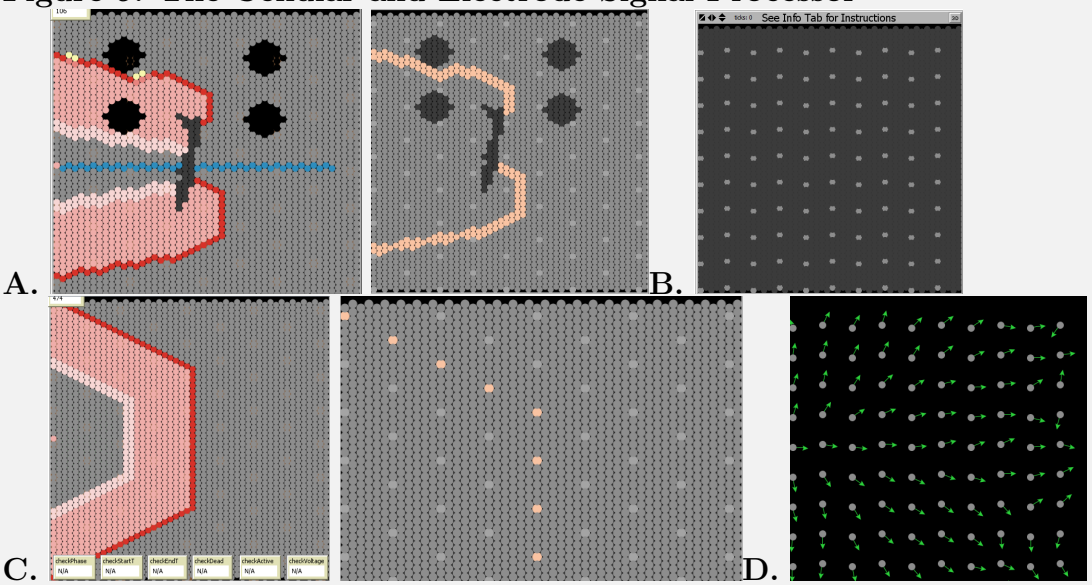

A. The configuration in the simulation creates a wave pattern that can be recorded through its active times and loaded onto the Therapy Guidance program.

B. Electrodes can be patterned into squares for a specific kind of sorting algorithm.

C. The shape of the wave of the simulation can be loaded up and converted into electrode information on the Therapy Guidance program.

D. The arrowhead option allows the user to see the direction of the wave of each electrode. This was done by measuring its vector in relation impacted by all of the other cells.

The activation files are in the form of a .txt file. They list all of the individual cells and each of the tick numbers of when they are triggered. The user is able to start and stop acquiring the cell activation times at any time and thus could end in the middle of a cycle, not capturing the full final wave across the atrium. These activation files can then be loaded into another program that just displays what the wave looks like based on these activation times. **Figure 9A** demonstrates this conversion. In this program, each individual cell does not have a behavior or individual properties as they did in the previous program. They only hold one variable, which is a list of activation times. Through this, it is assumable that cells with an empty list of activation times are dead or nonexistent, given that the recorded data is representative of one or more pulses.

Targeting Faulty Cells Using Cellular Voltage Data

We are now able to create an algorithm that can identify and target sick cells to kill. It can completely fix the identified rotors or spirals that are created as a result a particular configuration of cells, which is based only on the cells' activation times. This method works almost flawlessly and would only require killing the cells that need to be killed to solve the issue, instead of inefficiently cutting off a whole region of tissue. We begin the algorithm by determining the number of times, on average, a random cell activates in the recording. Keep in mind that this is not representative of the healthy number of pulses that were meant to occur, because bad waves could've passed over it even if the cell itself is good. Finding the random cell to choose requires some filtration. Since the user acquiring the electrical information could stop the program and save the activations at any point in time, there could be a discrepancy between the number of times activated between cells that were reached by the last wave and cells that were not. Since the area inside the last wave is where the problem is assumed to come from, we want to choose the random cell to be on that last wave. We find the max activation time and pick a random cell with that max activation time in its list of activation times. We call this the Basis Cell because it will be the basis for the number of activation times a healthy cell is supposed to have. In fact, the number of times the basis cell pulses is then called the "normal" number of pulses. The last activated cells are marked as dark green or orange.

Now that we have the number of normal pulses in the problematic animation, we can look for responsible cells. The best way to approach the problem is to examine the ways a bad cell could behave. The first possibility is that the cell acts as a Bad Node. This would mean that its cycle time is unusually short and it retriggers at a faster pace than the SA node does. Since bad nodes create their own pulses of waves, we may assume that at least one of the possible basis cells are on this bad wave. Thus, we can trace back recursively from the basis cell to find the origin of the bad wave. This can be done by checking the cell's neighbors and applying the recursion to all of the cells that have a slightly lower activation time within that pulse. Then these cells would do the same thing over and over again, directing the function to a new cell every time until it comes to a cell where there are no longer any neighbors with near earlier activation times (not drastically earlier, since drastically lower activation times will probably mean that it is from the previous wave). Since the basis cell is at the edge of the last wave and the cells outside of the last wave are bound to have a drastically lower last activation time, I've made it so that the recursion cannot continue down a path if the current cell has fewer pulses than normal. This also stops the path from following faulty

cells.

Figure 10. The Development of Rotors through a specific Configuration of Cells

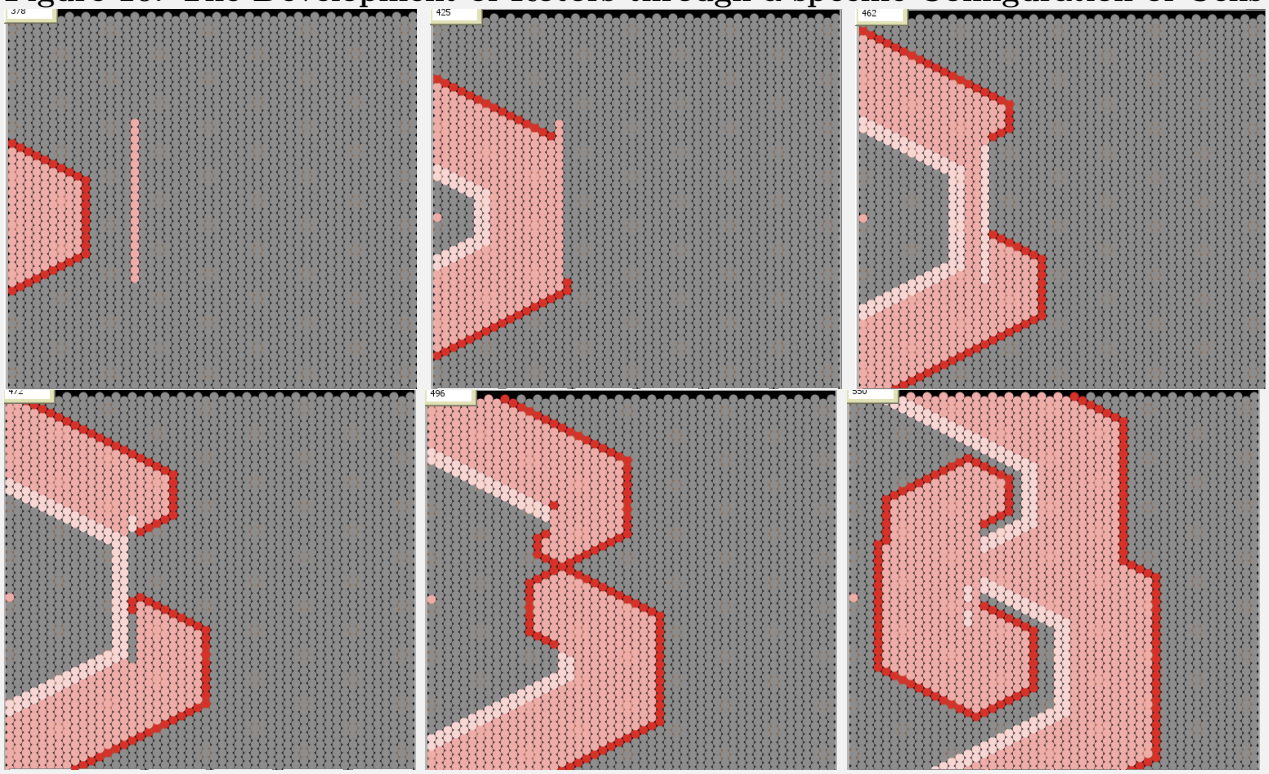

This example demonstrates how a group of sick cells can create a rotor without directly creating bad waves. Here, a wave loops around a line of cells still in their hold phase and breaks through in the middle of the line when the sick cells go back to their rest phase. This creates two rotors around the line of sick cells, and consequently, an extra wave.

Finally, since two nodes can create waves that coexist and eventually converge, the algorithm sometimes detects the trigger from the SA node path (left center in animation), where the basis node's wave comes directly from the SA node. However, since there must exist at least one cell that is part of the bad wave given that there exists a bad node, the algorithm keeps trying until it finds a wave that is not from the SA node source. Additionally, the user can optionally choose to go through every possible basis cell, in case there is more than one bad node. Thus, after all possible attempts, the program succeeds in finding the bad cell acting as a node. This Bad Node algorithm will also succeed in detecting the faulty cells that cause the arrhythmias directly (as opposed to creating a rotor or spiral), because they ultimately create their own bad waves.

Another possibility is that bad cells, rather than directly creating the bad waves, create rotors or spirals that cause the fibrillation. See **Figure 10** to understand how this happens. Although these cells are sick, they don't directly cause the reentering wave, so the Bad Node algorithm will

not detect them. However, they still can be detected by a second algorithm. Since these cells still have abnormal phase times, although they are not directly responsible for the irregular pulses, their behaviors will be different from those of healthy cells. It is assumable that in order to create the rotors and spiral waves, these cells do not activate when they are supposed to at certain points in the recording. This assumption comes with the fact that rotors and spirals must be caused by a dynamic disruption in the flow of the wave.

Thus, these sick cells can be targeted by comparing the normal pulse amount to the pulse amounts of every possibly sick cell. If a living cell pulses a lesser number of times than the normal pulse amount, then it must be a cell that broke through one or more of the waves that passed over it without activating. This could be due to a longer Hold Phase or Fall Phase. We then check if there is ever an occasion where the cell should have been triggered by its neighbors but wasn't. To do this, we compare the activation times of the potentially bad cell to that of its neighbors. 10 ticks, in this case, is a reasonably sufficient amount of time to say that a cell should be triggered by its neighbor, given randomness and bundle influence. We can then mark these cells that were supposed to trigger, but didn't, as sick. **Figures 11A, 11B** and **12A** show a few sample results from running this algorithm.

One rare case occurs when a cell with a long rise time or delayed rise time works together with other sick cells of various configurations to create a rotor. This would be different because the faulty cell technically directly starts the bad wave while also creating a rotor. This would be treated the same way as the algorithm treats cells acting as nodes, as it is essentially causing the reentry. Therefore, the node detection algorithm would identify and target the cell. Finally, the Peak Phase would never realistically be non-instantaneous, so there is no need to worry about its effect on the behavior of a cell. Therefore, that settles all possible irregularities that could occur in the phase times of individual cells.

Figure 11: Therapy Guidance of Cellular Information and Fill-In Algorithm

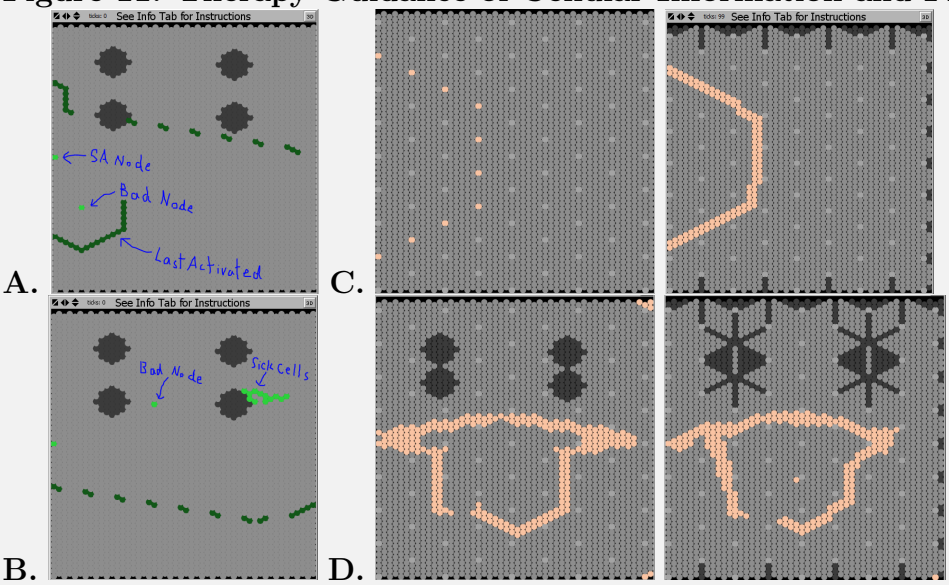

A. C.

B. D.

A. The algorithm for finding a bad node starts sometimes finds the SA node if the last activated wave comes directly from the SA node. In this case it will try another basis cell.

B. The algorithm for finding cells with bad phase times looks for cells that pulse a different number of times than the number of waves that pass it.

C. Cells in between each of the activated electrodes are filled through the fill-in algorithm.

D. This is the comparison between pure cellular data and filled in electrode data.

Of course, there is the possibility that the chosen basis cells happens to be the sick one. Since it would have more or less numbers of activation than the healthy cells, it would mark as sick, every other cell, except for the ones that activated the same irregular amount of times as itself. This, however, would be very obvious, as every single one except for the few sick ones would be targeted. Thus, the algorithm keeps trying again until it finds a realistic solution.

In the end, almost all of the bad cells that cause the problem are successfully targeted. There sometimes are some few excess bad cells that are not causing any problems that are targeted as well, because the second algorithm may find a few other oddly acting cells. However, killing these too, though not entirely efficient, would not make a difference in the structure of the heart, as seen by the current much less efficient methods. Compared to the millions of healthy excess cardiac cells killed in the process of ablation, the relatively few excess cells killed in the auto-ablation algorithm have virtually no impact. Thus, the Therapy Guidance algorithm has an almost perfect success rate and still does very little damage to the tissue of the heart.

The Detection of Faulty Cells Using Electrode Data

The algorithm works with cellular data, but realistically has to get passed the physical restriction with resolution. Though able to automatically target and kill cells that cause devastating rotors that affect millions today, curing them of their fibrillation, as described, the program would require the activations of every cell, in the order of 10,000 cardiac cells. In reality, technology and engineering have not progressed enough to be able to measure every cell's voltage vs. time. Instead, doctors use electrodes to measure an array of small patches of cells. The highest resolution of these electrodes that companies are able to produce is still in the order of 1 mm patches separated by a few millimeters, which would cover in the order of millions of cardiac cells separated by a few times that. In order to make the algorithm work with this sparse, less precise electrode information, some sophisticated estimation must be done in order to convert this into a more connected map of cellular information. This approach is known mathematically as the Inverse Problem. Taking a less pixelated view and increasing its resolution would be guesswork and almost impossible. However, in this particular case, it is much more achievable due to the fact that bad nodes, rotors, and spirals create waves outward, instead of in the direction of the spiral. In other words, even if there were a rotor completely hidden somewhere in between electrodes, the fact that it creates waves that grow outward means that it will eventually reach nearby electrodes.

Thus, we add a model of a hexagonally patterned electrode map onto the simulated cellular automaton. Each of these electrodes measure only the voltage and activation time of the cell that is under it. Then, we add the ability to save activation times that only these electrodes pick up, and place them into the Therapy Guidance program.

Algorithm for Approximating Cellular Information from Electrode Information

Figure 12: Barycentric Interpolation and the Trace-Back Algorithm for Finding a Bad Node

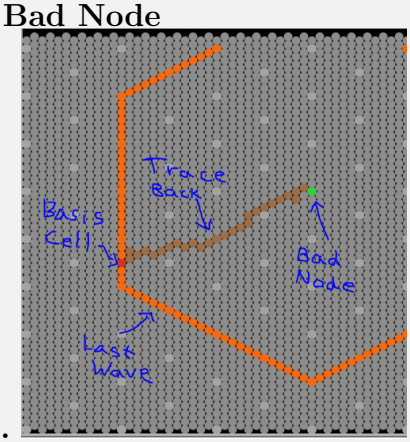

A.

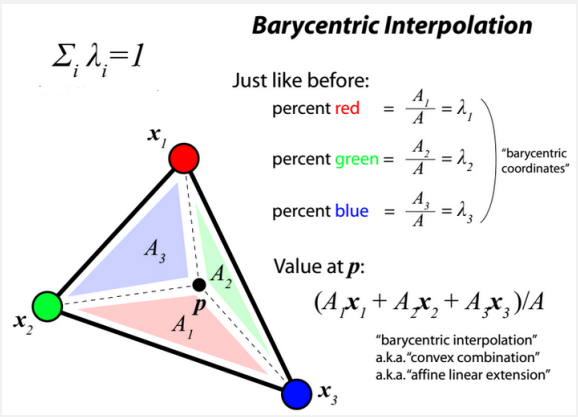

B.

A. The solution shows where the animation of the arrhythmia's faulty waves is stopped. Then, it randomly chooses a basis cell from the last wave and traces backwards toward the bad node. This works for every problem not caused by a rotor or spiral but by a bad reentering cell.

B. Barycentric Interpolation finds the weight of each point on a triangle on a position in the middle of the triangle by comparing the areas on the opposite side of the point.

From this program, only a subset of activations from cell under an electrode is available and the goal is to convert this into an approximation of the activations for all of the other cells (in between electrodes). Each cell has to take into account the effect of each of its surrounding electrodes' voltages. Since any arrangement of electrodes can be formed into triangles, the conversion can be accomplished through a theory called Barycentric Interpolation. This gives a value to a cell in between two or three other points by determining its weighted contribution from each of those points, depending upon how far the cell is from each. **Figure 12B** shows how the point is affected in Barycentric Interpolation. For simplicity, the electrodes are in a hexagonal pattern, so that it imitates the cell's hexagonal setup. Using Triangular Barycentric Interpolation, we can find the activation times for all cells in between 3 electrodes of a triangle. I've implemented this through the "Fill-In" algorithm, demonstrated in **Figure 11C** and **11D**. There are a few cases near the edge of the grid and near dead or hole cells where the electrode has no voltage readings, and these may impede the calculation of the Barycentric Interpolation in those areas. To fix this problem, the fringe cells that are potentially affected are set as dead, explaining the weird pattern of dead cells when

running the Fill-In Algorithm. Otherwise, comparing the pure cellular recordings with the estimated values based on electrode information, the Fill-In algorithm depicts the cellular information quite accurately.

Conclusion

All in all, the "filled in" cellular data successfully goes through the Therapy Guidance algorithm. Thus, the entirety of the program is able to target and fix faulty cells through just electrode measurements. The end product of this program would be one where doctors take information from electrodes in a patient's heart and plug these into the program, which would automatically target and guide ablation of specific cell areas that are causing cardiac rotors and spirals. This is not only much more efficient than current ablations, but it also has a much higher success rate and erases the possibility of human error in curing irregular or rapid heartbeats.

Future Improvements

The next steps to take would be to use the algorithm on real-life data. The auto-ablation algorithm works so far on artificially reconstructed data from a simulation of an arrhythmia. Thus, in theory, if the simulation accurately depicts what happens in the electrophysiology of the left atrium, the procedure should work on a real heart. Unfortunately, real electrode readings from sick patients are difficult to obtain without correct permissions. In addition, this program would only work specifically with endocardial electrode readings. Pericardiograms and Surface ECGs will not provide the appropriate information, since they are measured from outside of the heart and from the outside of the chest, respectively. Finally, a new rising engineering technology of patterned electrodes like the one in the program would be more suitable for the algorithm. However, it is also possible to use the algorithm with randomly scattered electrodes as long as their relative positions are recorded. This has been accomplished today by NavX or Carto since it is easy to incorporate into the program.

References

[1] Berrut, Jean-Paul, and Lloyd N. Trefethen. "Barycentric Lagrange Interpolation." SIAM Review 46.3 (2004): 501. Web.

[2] Cochet H., R. Dubois, F. Sacher, N. Derval, M. Sermesant, M. Hocini, M. Ontaudon, M. Haissaguerre, F. Laurent, and P. Jais. "Result Filters." National Center for Biotechnology Information. U.S. National Library of Medicine, Apr. 2014. Web. 29 Sept. 2014.

[3] Delisle, Brian P., Blake D. Anson, Sridharan Rajamani, and Craig T. January. "Biology of Cardiac Arrhythmias." Biology of Cardiac Arrhythmias. American Heart Association, 2004. Web. 26 June. 2014.

[4] Gomez-Gesteira M., J.L Del Castillo, M.E Vazquez-Iglesias, V. Perez-Munuzuri, and V. Perez-Villar. "Influence of the Critical Curvature on Spiral Initiation in an Excitable Medium." Physical Review E. The American Physical Society, 1 Aug. 1994. Web. 22 Aug. 2014.

[5] "NetLogo Home Page." NetLogo Home Page. N.p., n.d. Web. 12 Nov. 2014.

[6] Pandit, Sandeep V., and Jose Jalife. "Rotors and the Dynamics of Cardiac Fibrillation." Circulation Research. American Heart Assiociation, 2012. Web. 9 Aug. 2014.

[7] "Beta Blog." : Genetic Modification Yields Biological Pacemakers. N.p., n.d. Web. 20 Sept. 2014.

[8] "Heart Arrhythmia." Mayo Clinic. Mayo Clinic, n.d. Web. 29 Sept. 2014.

[9] "Surgeon Q&A: Dr. T. Sloane Guy Helps Kerrigan, Simone & Tina." Adams Heart Valve Surgery Blog Surgeon QA Dr T Sloane Guy Helps Kerrigan Simone Tina Comments. N.p., n.d. Web. 20 Sept. 2014.

[10] "The Heart of ICU." The Heart of ICU. N.p., n.d. Web. 20 Sept 2014.

4 Categorizing Point Sets with No Empty Pentagons

by George Drimba

Abstract

Motivated by a question proposed by David R. Wood, we attempt to categorize finite point sets that do not have a 5-hole (*empty pentagon*). We look at a finite set of points, P, and consider the case that these points are in strictly convex position. We use the Erdős-Szekeres Theorem in tandem with a construction of convex layers and the visibility graph of the point set to extract information regarding the existence of an empty pentagon. A second approach is taken using the Djoković-Winkler relation to check if the flip graph of the point set is isometric to a hypercube, thereby verifying if the point set has an empty pentagon. We attempt to construct sets such that the Djoković-Winkler relation is an equivalence relation, creating point sets with 5-holes. We then propose an extension of the Erdős-Szekeres Theorem into higher dimensions.

Introduction and Fundamental Notions

Terminology

We begin by defining some of the terminology necessary to discuss empty pentagons and other facets of computational geometry. We let P be a finite set of points in the plane. If no three points in P are collinear we say that the set P is in general position. We let $\text{conv}(P)$ denote the convex hull of P. We let S be a vector space over any ordered field. A set $C \in S$ is convex if for each $x, y \in C$ and $t \in [0, 1]$, the point $(1-t)x + ty$ is in C. For a finite point set with N points, $p_1, p_2, \ldots, p_N$, we have $\text{conv}(P) = \{\sum_{j=1}^{N} \lambda_j p_j : \lambda_j \geq 0 \, \forall \, j \, and \sum_{j=1}^{N} \lambda_j = 1\}$. The convex hull of a point set is the intersection of all the convex sets containing those points. This definition can be extended from the typically discussed Euclidean Space, to any arbitrary real vector space. The common analogy used to visualize the convex hull is a rubber band stretched around the desired point set.

Definitions

We say that P is in convex position if every point of P is on the boundary of $\text{conv}(P)$, denoted $\partial \text{ conv}(P)$. A point x $\in P$ is said to be a corner of P if $\text{conv}(P - x) \neq \text{conv}(P)$. We say P is in strictly convex position if each point of P is a corner of P. A strictly convex k-gon is the convex

hull of k points in strictly convex position. If $X \subseteq P$ is a set of N points in strictly convex position and $\text{conv}(X) \cap P = X$, then we say $\text{conv}(X)$ is a *N-hole*. In essence, we have a *N-hole* when X forms the vertices of a convex polygon which does not include any other points of P. We define the diagonal of P to be a line segment such that $P \cap Conv(\{a, b\}) = \{a_0, a_1\}$, thereby forming an empty $2 - gon$. A *visibility graph* of a point set P has vertex set P and $P_i, P_j \in P$ are adjacent if and only if they are visible with respect to P, that is if they are a diagonal of P (a diagonal is an edge of the viability graph).

Geometric Elements

A triangulation of P is any graph with a vertex set of P and an edge set comprised of the maximal set of diagonals that do not cross each other. Therefore a triangulation is a division of a surface or plane polygon into a set of triangles, with the restriction that each triangle side is entirely shared by two adjacent triangles. Since our finite point set in a Euclidean space is closed and bounded, it follows that it is compact by the *Heine-Borel* Theorem. Hence, our point set can be triangulated with finitely many triangles as shown by Francis and Weeks (1999).

We will now proceed to define two graphs for a finite point set P that will later be implemented. The *Quadrilateral Graph*, denoted as $QG(P)$, is defined to be a graph with a vertex set corresponding to the diagonals of P (each vertex of $QG(P)$ represents a diagonal of P). Diagonals $a_i a_j$ and $b_k b_l$ are connected (represented by the vertices a and b respectively) whenever the segments $\overline{a_i a_j}$ and $\overline{b_k b_l}$ intersect and $\{a_i, a_j, b_k, b_l\}$ are the vertex set of an empty quadrilateral. The *Flip Graph*, denoted as $FG(P)$ is the graph with a vertex set corresponding to the triangulation of P (each vertex of $FG(P)$ represents a triangulation of P) where two vertices are adjacent if the triangulations that they represent have a flip distance of 1 (which is the removal of one diagonal that is then replaced by another). It should be noted that we define the flip distance between two triangulations as the number of flips (diagonal replacements) needed to transform one triangulation into another.

Theorems, Lemmas and an Approach

We will begin by providing and developing some of the machinery used to dealt with the aforementioned problem. The following theorem of Erdős and Szekeres will be crucial to our explorations.

Theorem 1. *For every $n \in \mathbb{Z}$, where $n \geq 3$, there exists a minimum integer that we will denote as $ES(n)$, such that every set of $ES(n)$ points in general position contain n points that are the vertices of a convex n-gon (they are in strictly convex position).*

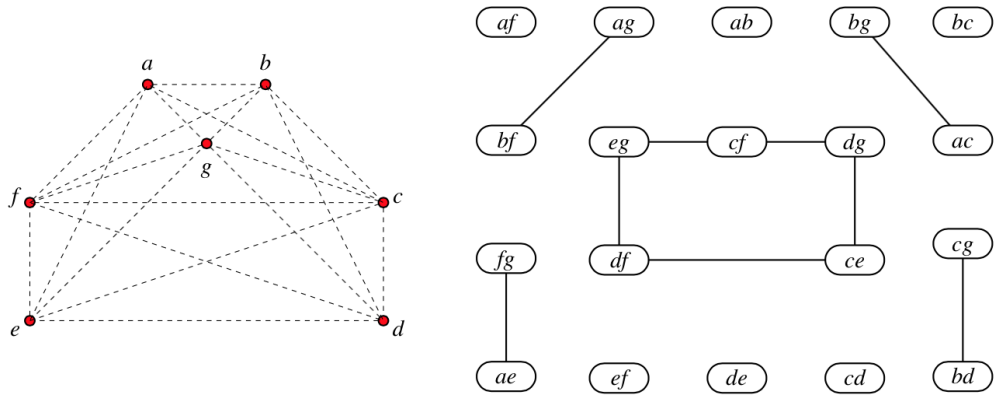

Figure 1: An example of a quadrilateral graph

It should be noted that $ES(n)$ is not known to have an explicit form however the following bounds have been proven: $ES(n) \geq 2^{n-2} + 1$ and $ES(n) \leq \binom{2n-5}{n-2} + 1$ when $n \geq 7$.

Problem 1. *For every $n \in \mathbb{Z}$, where $n \geq 3$ determine the smallest positive integer $H(n)$ (if it exists), such that any set P of at least $H(n)$ points in general position in the plane contains n points which are the vertices of an empty convex polygon (n-hole).*

The case $n = 3$ or $n = 4$ is trivial, hence $ES(3) = 3$ and $ES(4) = 5$. Harborth showed that, for every finite set of ten or more points in general position in the plane, some five of them form an empty convex pentagon, hence we can restrict our set to less than ten points as $H(5) = 10$ as we know that any set with ten or more points will have an empty pentagon.

Theorem 2. *For all $l, k \in \mathbb{Z}$, where $l \geq 2$ and $k \geq 3$, $\exists$ a minimum integer, $ES(k, l)$ such that every set of $ES(k, l)$ in a plane contains l collinear points or k points in strictly convex position. (This theorem that can be attributed to [7]).*

Using theorem 1 and 2 we attempted to show that every set of $ES(\frac{(2l-1)^l - 1}{2l-2})$ for any $l \in \mathbb{Z}$,l >2, contains l collinear points or a 5-hole. For the sake of contradiction we assumed that the set of $ES(\frac{(2l-1)^l - 1}{2l-2})$ points had no empty pentagon and no l points, that are collinear. We then attempted to use convex layers to prove the conjecture. We defined the outermost convex layer, C_1 to be the k-minimal subset of our point set, meaning there is no set of at least k points such that $conv(X) \subsetneq conv(C_1)$. We then defined the subsequent layers recursively as follows: $C_l := p \cap \partial conv(p \cap int(conv(C_{l-1}))$. This method of defining the layers was not fruitful in obtaining the desired contradiction. It was found that a similar approach was taken by [1], however this

approach lead to much more successful ends as the layers were defined in a different manner, allowing a contradiction to be yielded and the conjecture to be proven.

A Geometric Approach

We will now provide equivalent conditions that have been proven to be true for a finite point set. We will explain the machinery needed to embark on this approach and then expound on a possible solution to the problem as well as a failed attempt.

Theorem 3. *The following conditions are equivalent for a finite point set P*

1. *P has no empty pentagon*
2. *The quadrilateral graph of P is a forest*
3. *The flip graph of P is a partial cube*

A forest is an acyclic graph that consists only of trees that could be possibly disconnected. While the second property could garner results we will proceed to focus on the third, hoping to yield a method for generating sets without an empty pentagon. A partial cube, which we shall denote as $\mathscr{H}(X)$ is an isometric subgraph of a hypercube. Hence, a partial cube is a subgraph of an a hypercube that preserves distances- where the distance between two vertices in the subgraph is the same as the distance between those two vertices in the hypercube. $\mathscr{H}(X)$ can be labeled with bit strings of equal length such that the Hamming distance between two vertices in the graph is equal to the Hamming distance between their labels. Hence we can say that the Hamming labeling represents an isometric embedding of the partial cube into a hypercube.

We will now proceed to introduce one of the essential techniques that we can use to characterize partial cubes. The Djoković-Winkler relation, denoted as Θ, states that $e_1 \Theta e_2$ where $e_1 = \{x_1, y_1\}$ and $e_2 = \{x_2, y_2\}$ if $d(x_1, x_2) + d(y_1, y_2) \neq d(x_1, y_2) + d(x_2, y_1)$. It is obvious that the aforementioned relation is symmetric and reflexive however it is not an equivalence relation (take $K_{2,3}$ for instance). In the case that a graph is bipartite and Θ is transitive then that graph is a partial cube. Using the computational power of a computer, it was attempted to generate random flip graphs that would satisfy the Djoković-Winkler Equivalence Relation- thereby generating sets with no empty

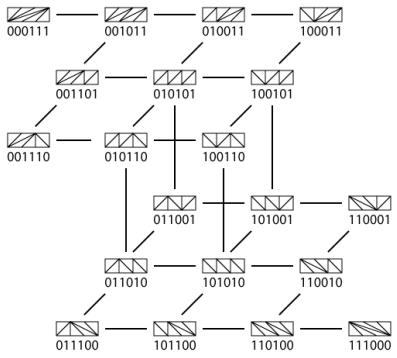

Figure 2: An example of a flip graph for a 2 x 4 grid.

pentagons. Since our flip graphs have vertices that correspond to triangulations, the vertex set of our graphs can be bounded.

The Catalan numbers, which we define by the following: $C_0 = 1$ and $C_{n+1} = \sum_{i=0}^{n} C_i C_{n-1}$ for $n \geq 0 \Rightarrow C_n = \frac{1}{n+1}\binom{2n}{n}$ will serve to provide a bound for our problem. It is well known that the nth Catalan number counts the triangulations of an $n-2$ convex polygon; hence we can bound the vertex set of our graph to having no more than $C_7 = 429$ vertices. The time and computational power to generate many of these flip graphs is not available. However we propose the following approach to categorizing the point sets with no empty pentagon: construct sets that satisfy the Djoković-Winkler equivalence relation rather than attempt to recognize some overarching pattern or characteristic that is pertinent in sets with no empty pentagon. This approach will be further pursued and has now taken center stage of our research.

Discussion and Higher Dimensional Extensions

The methods discussed and implemented in this paper are of contemporary significance. Many open problems remain in the field of computational geometry and many deal with the idea of sets without empty convex polygons. Much of the theory and machinery developed in order to deal with problems involving k-holes remains unchanged for a rather lengthy period of time. Since the proposal of the original Erdős and Szekeres problem, the techniques used to solve problems of this nature involve bounds proved using cups and caps (which were not discussed in this paper). The notion of using cups and caps has been useful when these points are in a plane however it has been shown that an extension of the Erdős and Szekeres theorem to higher dimensions will require a different approach. Using Θ to construct bipartite flip graphs would enable us to generate graphs that do not have an empty pentagon- providing a much easier way to categorize our point sets. We

also desire to propound the idea of extending the notion of the flip graph to higher dimensional analogues much in the same manner as $d - dimensional$ Delaunay triangulations; allowing us to categorize points sets in any Euclidean space that do not have an empty polytope. By extending the idea of general position in $\mathbb{R}^n$ to the property that no $n+1$ points lie on the same hyperplane, we can attempt to extend Erdős and Szekeres's theorem to higher dimensions. We consider the set, $S \in \mathbb{R}^n$ of $ES_2(k)$ points (note that the subscript represents the dimension, in general we have $ES_n(k)$ representing the minimal number of points in $\mathbb{R}^n$ such that every set of $ES_n(k)$ has k points in convex position) and its projection T onto a subspace of $\mathbb{R}^n$ such that T is in general position in this subspace. Since we know that the $|T| \geq ES_2(k) \Rightarrow$ there are n points in convex position that can be found in T (causing its preimage in S to also be in convex position) allowing us to extend Erdős and Szekeres's to higher dimensions. Hence we can extend this technique to any dimension less than n, leading to the inequality $ES_n(k) \leq ES_{n-1}(k) \leq \cdots \leq ES_2(k) \leq \binom{2n-5}{n-3} + 2$.

References

[1] Zachary Abel, Brad Ballinger, Prosenjit Bose, S Ebastien, Collette, and ? Ferran Hurtado, Scott D. Kominers, Stefan Langerman,. "EVERY LARGE POINT SET CONTAINS MANY COLLINEAR POINTS OR AN EMPTY PENTAGON." (n.d.): n. pag. Web.

[2] Geometry, Journal Of Computational. Distance in Such Point Sets Can Be Computed Efficiently. (n.d.): n. pag. Web.

[3] Elekes, G. A Combinatorial Problem on Polynomials. Discrete and Computational Geometry 19.3 (1998): 383-89. Web.

[4] Eppstein, David. "Cubic Partial Cubes from Simplicial Arrangements." (n.d.): n. pag. Web.

[5] Francis, G. K. and Weeks, J. R. "Conway's ZIP Proof." Amer. Math. Monthly 106, 393-399, 1999.

[6] Horton, J. D. "Sets with No Empty Convex 7-gons." CMB:. N.p., n.d. Web. 12 Nov. 2014.

[7] Jiri Matousek. Lectures on Discrete Geometry, vol. 212 of Graduate Texts in Mathematics. Springer, 2002. ISBN 0-387-95373-6.

[8] Ovchinnikov, Sergei. "Partial Cubes: Structures, Characterizations, and Constructions." Discrete Mathematics 308.23 (2008): 5597-621. Web

[9] Pinchasi, Rom, Rados Radoici C, and Micha Sharir. "On Empty Convex Polygons in a Planar Point Set." Journal of Combinatorial Theory (n.d.): n.

[10] Rabinowitz, Stanley. Consequences of the pentagon property. Geombinatorics, 14:208-220, 2005.

[11] Valtr, Pavel Convex independent sets and 7-holes in restricted planar point sets. Discrete Comput. Geom., 7(2):135-152, 1992.

5 Proofs Without Words

by Sophia Zheng and Amanda Wang

Sine of Sum. Let $r = \frac{1}{2}$.

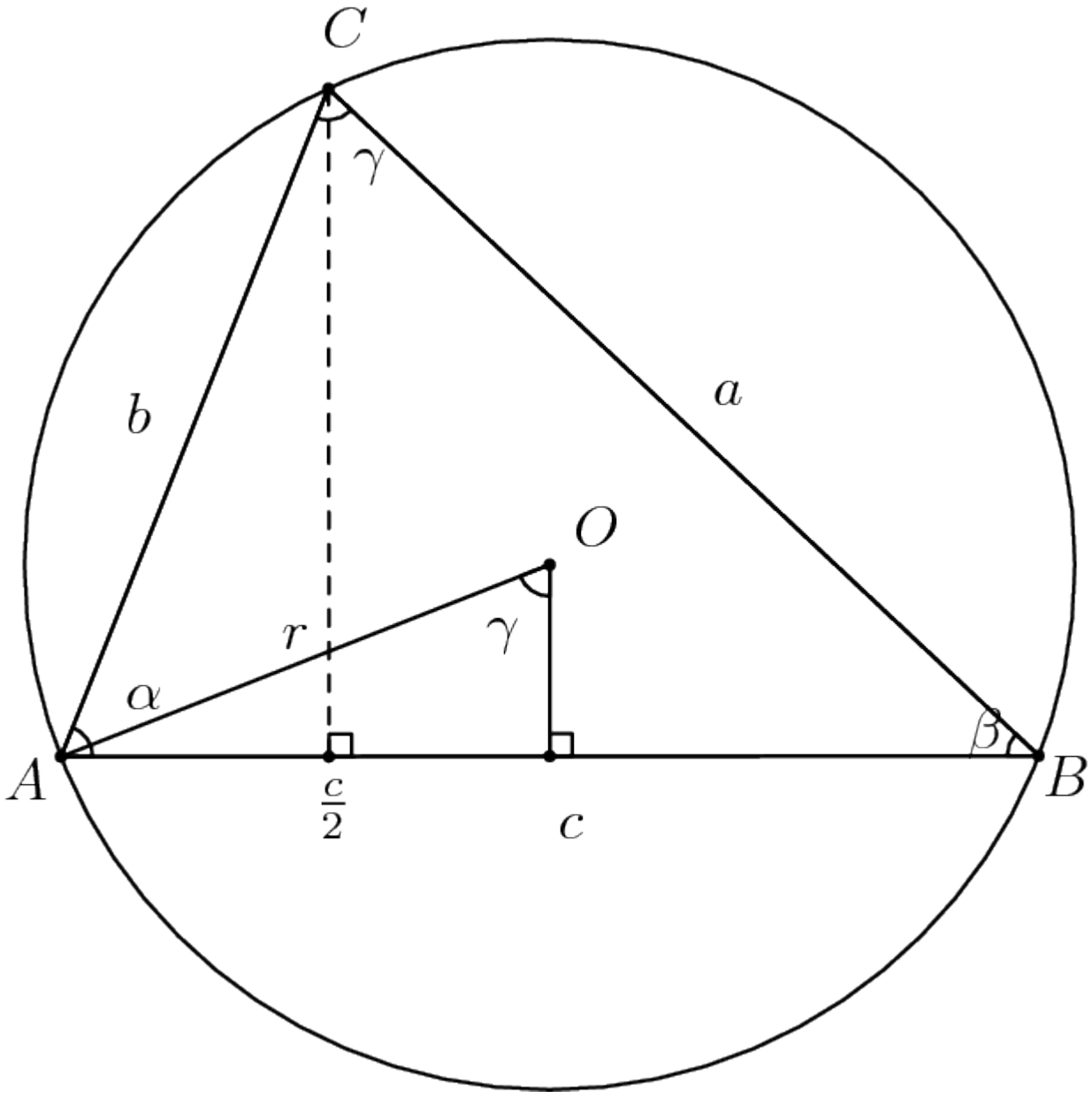

$$c = a\cos\beta + b\cos\alpha;\ \ \sin\gamma = \frac{\frac{c}{2}}{\frac{1}{2}} = c,\ \ \sin\alpha = a,\ \ \sin\beta = b$$

$$\sin(\alpha+\beta) = \sin(\pi - (\alpha+\beta)) = \sin\gamma = c = \sin\alpha\cos\beta + \cos\alpha\sin\beta$$

QM-AM-GM-HM Inequality

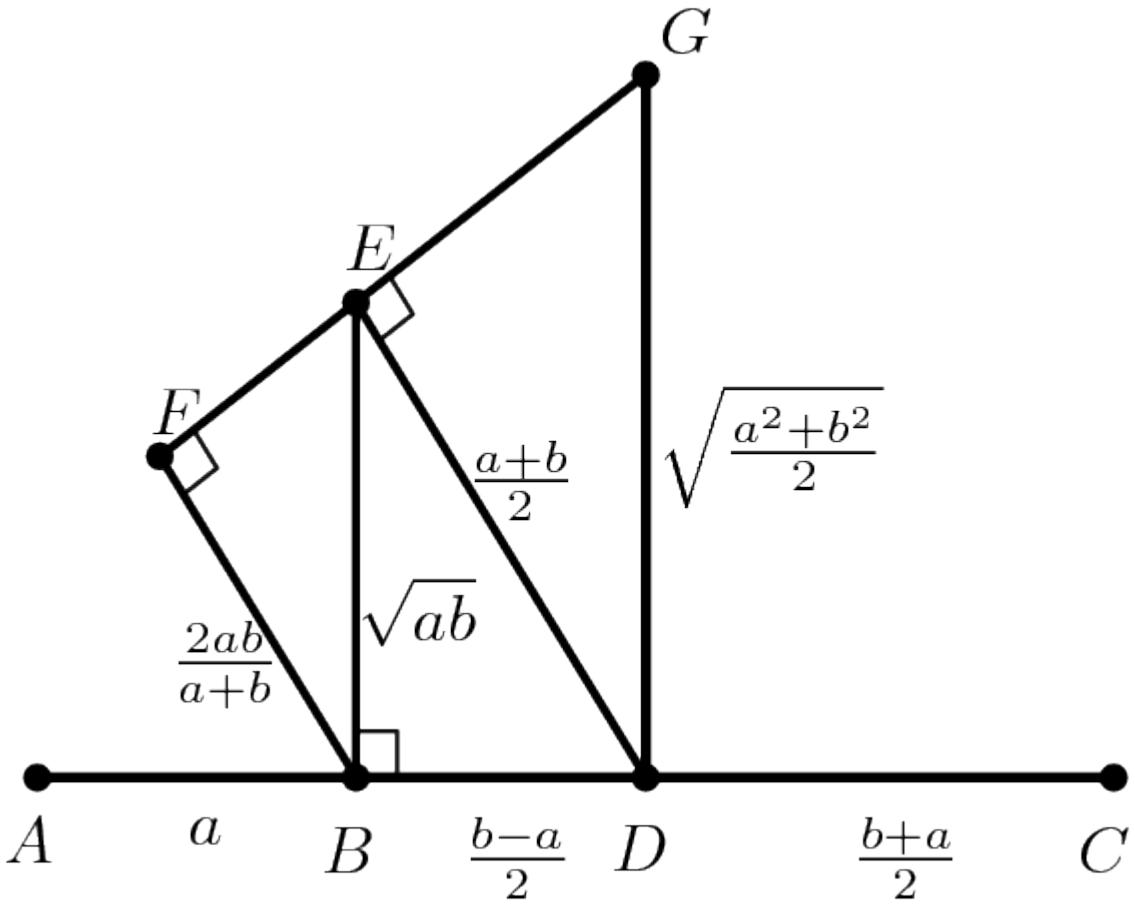

$AB = a,\ BC = b$

$AD = DC = \dfrac{a+b}{2}$

$BE \perp AB,\ DE = AD$

$FE \perp ED,\ FB \parallel ED$

$EG = BD = \dfrac{b-a}{2}$

6 Problems

Curated by Max Fishelson and Calvin Lee

Problem 1. Triangles ABC and ABD are isosceles with $AB = AC = BD$, and BD intersects AC at E. If BD is perpendicular to AC, then $\angle C + \angle D$ is

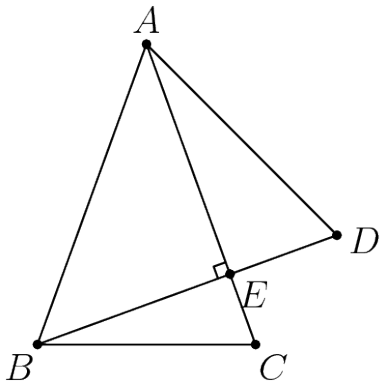

(A) 115° (B) 120° (C) 130° (D) 135° (E) not uniquely determined

Problem 2. Find the remainder when $9 \times 99 \times 999 \times \cdots \times \underbrace{99\cdots9}_{999\text{ 9's}}$ is divided by 1000.

Problem 3. Let z be a complex number with $|z| = 2014$. Let P be the polygon in the complex plane whose vertices are z and every w such that $\frac{1}{z+w} = \frac{1}{z} + \frac{1}{w}$. Then the area enclosed by P can be written in the form $n\sqrt{3}$, where n is an integer. Find the remainder when n is divided by 1000.

Problem 4. Let n be a fixed positive integer. A group of n people stand in a circle, and are each randomly given a red or a blue hat. Each person can see everyone else's hats, but not their own. They are then simultaneously asked to guess the color of their own hat. If the people are allowed to strategize before the hats are distributed, and they win only if everyone guesses correctly, find the probability that they win (if they play optimally).

Problem 5. Let C be a circle and let P be a point in the exterior of C. The tangents from P intersect the circle at A and B. Let M be the midpoint of segment AP and N be the second intersection of the line BM with circle C. Prove that $PN = 2MN$.

Problem 6. Show that, for any fixed integer $n \geq 1$, the sequence

$$2,\ 2^2,\ 2^{2^2},\ 2^{2^{2^2}}, \ldots \pmod{n}$$

is eventually constant.

Problem 7. In equilateral triangle XYZ, we have points A, B, C, D, E, F going around the triangle with A and B on XY, C and D on YZ, and E and F on ZX such that hexagon $ABCDEF$ is equilateral (not necessarily equiangular). Prove that if we extend the sides of the hexagon BC, DE, FA (those not aligned with the sides of XYZ) they will form another equilateral triangle.

Problem 8. Let $S(n)$ be the maximum number of points we can have in n space where there are only two distinct pairwise distances between the points. (This means that for some real numbers d_1 and d_2, the distance between any given pair of points is either d_1 or d_2.) Show that

$$\lim_{n\to\infty} \frac{S(n)}{\frac{n^2}{2}} = 1.$$

Problem 9. Let ABC be a non-equilateral triangle and let M_a, M_b, M_c be the midpoints of the sides BC, CA, AB, respectively. Let S be a point lying on the Euler line. Denote by X, Y, Z the second intersections of M_aS, M_bS, M_cS with the nine-point circle. Prove that AX, BY, CZ are concurrent.

(Recall that the Euler line is the line passing through the circumcenter and orthocenter, and the nine-point circle is the circumcircle of M_a, M_b, and M_c.)

7 Solutions

by Max Fishelson and Calvin Lee

Problem 1. (AHSME) Triangles ABC and ABD are isosceles with $AB = AC = BD$, and BD intersects AC at E. If BD is perpendicular to AC, then $\angle C + \angle D$ is

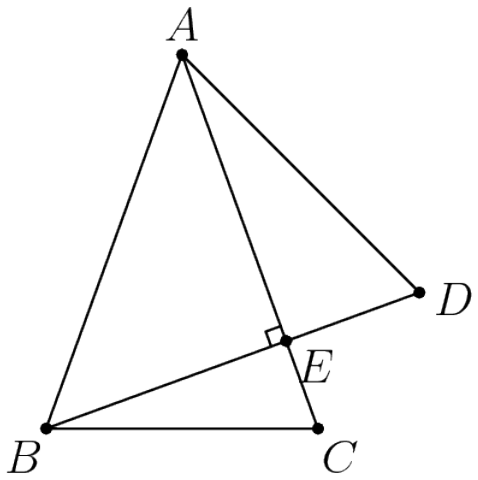

(A) 115° (B) 120° (C) 130° (D) 135° (E) not uniquely determined

Solution 1. Redraw the figure as a concave pentagon $ADECB$:

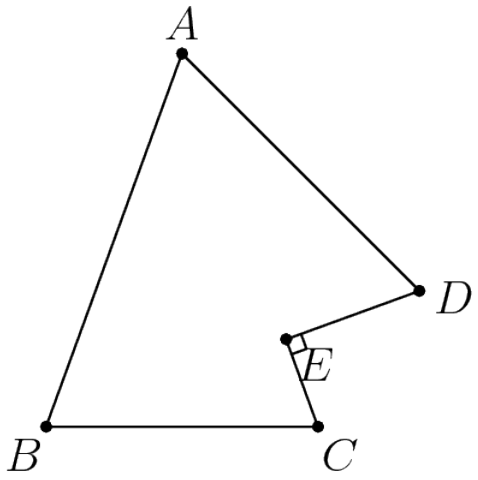

The angles of this pentagon sum to $180° \cdot 3 = 540°$. As a quick proof, note that the nine angles of three original triangles $\triangle AEB$, $\triangle CBE$, and $\triangle DEA$ all make up the angles of the pentagon without overlap.

Since reflex $\angle E = 270°$, we have

$$\angle C + \angle B + \angle A + \angle D = 540° - 270° = 270°.$$

From isosceles $\triangle ABC$, we get $\angle B = \angle C$. Similarly, from isosceles $\triangle ABD$, we know $\angle A = \angle D$. Substituting these into the equation above gives $2\angle C + 2\angle D = 270^\circ$. Therefore, $\angle C + \angle D = 135^\circ$, and the answer is $\boxed{\text{D}}$.

Problem 2. (AIME) Find the remainder when $9 \times 99 \times 999 \times \cdots \times \underbrace{99\cdots9}_{999\ 9\text{'s}}$ is divided by 1000.

Solution 2. Note that $999 \equiv 9999 \equiv \cdots \equiv \underbrace{99\cdots9}_{999\ 9\text{'s}} \equiv -1 \pmod{1000}$. That is a total of $999 - 3 + 1 = 997$ integers. When all of them are multiplied together, the result is congruent to $-1 \pmod{1000}$. Thus, the entire expression is congruent to $(-1)(9)(99) \equiv -891 \equiv \boxed{109} \pmod{1000}$.

Problem 3. (AIME) Let z be a complex number with $|z| = 2014$. Let P be the polygon in the complex plane whose vertices are z and every w such that $\frac{1}{z+w} = \frac{1}{z} + \frac{1}{w}$. Then the area enclosed by P can be written in the form $n\sqrt{3}$, where n is an integer. Find the remainder when n is divided by 1000.

Solution 3. We reduce the given equality:

$$\begin{aligned} \frac{1}{w+z} &= \frac{w+z}{wz} \\ wz &= (w+z)^2 \\ w^2 + wz + z^2 &= 0 \end{aligned}$$

Multiplying both sides by $(w - z)$ gives $w^3 - z^3 = 0$, i.e. $w^3 = z^3$. However, it is easy to see that $w \neq z$. Therefore, by DeMoivre's theorem, the values for w will be z rotated about the origin 60 and 120 degrees.

Let the two possible locations for w be W_1 and W_2 and the location of z be point Z. From the analysis above, we know W_1W_2Z is equilateral. There are many ways to finish from here; below, we present one which uses area.

Let x be the side length of the equilateral triangle. Since the circumradius of this equilateral triangle is 2014, we apply the formula $\frac{abc}{4R} = [ABC]$. Substituting the formula for the area of an equilateral triangle on the right hand side gives

$$\frac{x^3}{4R} = \frac{x^2\sqrt{3}}{4},$$

which yields $x = R\sqrt{3}$. Then the area is $\frac{x^2\sqrt{3}}{4} = \frac{3R^2\sqrt{3}}{4}$. Since we're concerned with the non-radical part of this expression and $R = 2014$, the answer is

$$\frac{3R^2}{4} \equiv 3 \cdot 1007^2 \equiv 3 \cdot 7^2 \equiv \boxed{147} \pmod{1000}.$$

Problem 4. Let n be a fixed positive integer. A group of n people stand in a circle, and are each randomly given a red or a blue hat. Each person can see everyone else's hats, but not their own. They are then simultaneously asked to guess the color of their own hat. If the people are allowed to strategize before the hats are distributed, and they win only if everyone guesses correctly, find the probability that they win (if they play optimally).

Solution 4. We first describe an optimal strategy which succeeds with probability $\frac{1}{2}$, and then prove that it is optimal.

Suppose everyone agrees beforehand that there will be an odd number of red hats. With this assumption, everyone can determine what their hat color is by counting the number of red hats they can see. If there actually is an odd number of red hats, which occurs with probability $\frac{1}{2}$, then everyone will be right; otherwise, everyone will be wrong. Thus, this strategy succeeds exactly half the time.

We can show that this is maximal by using linearity of expectation. Let E be the expected number of people who guess correctly. Look at any individual player, say Bob. Regardless of the strategy adopted beforehand, the probability that Bob guesses the color of his hat correctly is $\frac{1}{2}$, since Bob's hat is chosen randomly and independently from all the other hats. By linearity of expectation, no matter what the strategy is, $E = \frac{n}{2}$.

Suppose that there is a strategy which achieves a probability $p > \frac{1}{2}$. But then if we compute the E directly from the definition of expected value (not linearity of expectation), we find that E is a sum of nonnegative terms, one of which is $p \cdot n$, representing the situation where everyone guesses correctly. This forces $E > \frac{n}{2}$, contradiction. Therefore, this strategy is optimal.

Problem 5. (Virgil Nicula, AOPS Forum) Let C be a circle and let P be a point in the exterior of C. The tangents from P intersect the circle at A and B. Let M be the midpoint of segment AP and N be the second intersection of the line BM with circle C. Prove that $PN = 2MN$.

Solution 5. By Power of a Point, $MN \cdot MB = MA^2 = MP^2$. Hence, the line MP is tangent to the circumcircle of triangle PNB, which means $\angle MPN = \angle PBN$.

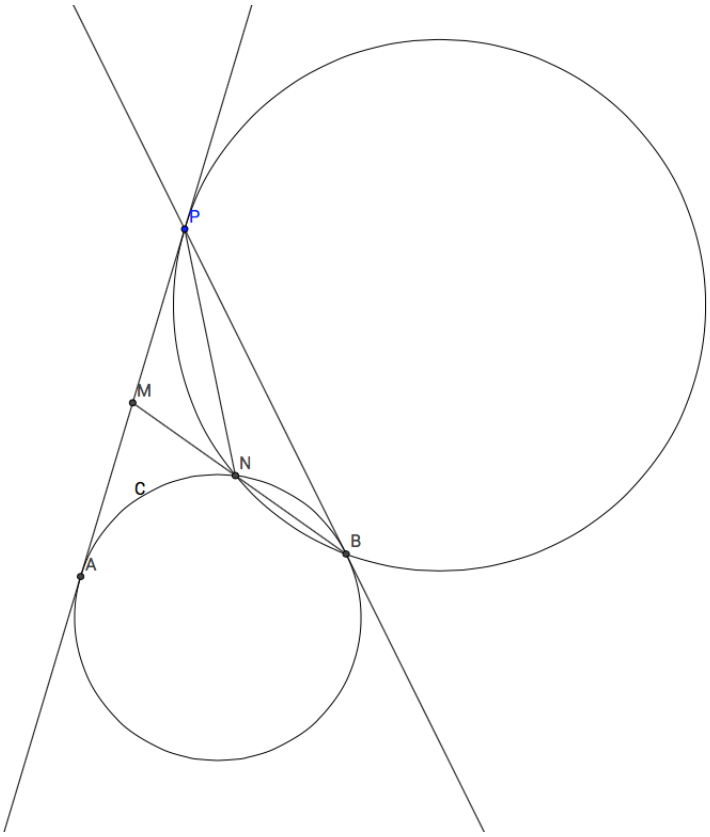

By Law of Sines, it follows that:

$$\begin{aligned}\frac{PN}{MN} &= \frac{PN}{\sin\angle PBN} \cdot \frac{\sin\angle PBN}{MN} \\ &= \frac{PB}{\sin\angle PNB} \cdot \frac{\sin\angle MPN}{MN} \\ &= \frac{PB}{\sin\angle PNB} \cdot \frac{\sin\angle PNM}{PM} \\ &= \frac{PB}{MN} = \frac{PA}{MN} = 2.\end{aligned}$$

This completes the proof.

Problem 6. (USAMO) Show that, for any fixed integer $n \geq 1$, the sequence

$$2,\ 2^2,\ 2^{2^2},\ 2^{2^{2^2}}, \ldots \pmod{n}$$

is eventually constant.

Solution 6. Suppose that the problem statement is false for some integer $n \geq 1$. Then we can choose the smallest n for which the statement is false; let this smallest value be b. Since all integers are equivalent mod 1, $b \neq 1$.

Note that for all integers b, the sequence $2^0, 2^1, 2^2, \ldots$ eventually becomes cyclic mod b. Let k be the period of this cycle. Since there are $k-1$ nonzero residues mod b. $1 \leq k \leq b-1 < b$. Since

$$2, 2^2, 2^{2^2}, 2^{2^{2^2}}, \ldots$$

does not become constant mod b, it follows the sequence of exponents of these terms, i.e., the sequence

$$1, 2, 2^2, 2^{2^2}, \ldots$$

does not become constant mod k. Then the problem statement is false for $n = k$. Since $k < b$, this is a contradiction. Therefore the problem statement is true, completing the proof.

Problem 7. In equilateral triangle XYZ, we have points A, B, C, D, E, F going around the triangle with A and B on XY, C and D on YZ, and E and F on ZX such that hexagon $ABCDEF$ is equilateral (not necessarily equiangular). Prove that if we extend the sides of the hexagon BC, DE, FA (those not aligned with the sides of XYZ) they will form another equilateral triangle.

Solution 7. The key idea is to use the properties of vector addition.

We see $\overrightarrow{AB} + \overrightarrow{BC} + \overrightarrow{CD} + \overrightarrow{DE} + \overrightarrow{EF} + \overrightarrow{FA} = \overrightarrow{0}$ since $ABCDEF$ is a closed polygon. Now, consider the vectors $\overrightarrow{AB}, \overrightarrow{CD}, \overrightarrow{EF}$. These three vectors all have the same length and the relative angles between them are 60 degrees. Hence, when we add $\overrightarrow{AB}, \overrightarrow{CD}, \overrightarrow{EF}$ together using head-to-tail vector addition, they form a closed equilateral triangle. Therefore $\overrightarrow{AB} + \overrightarrow{CD} + \overrightarrow{EF} = \overrightarrow{0}$.

Now, since $\overrightarrow{AB} + \overrightarrow{BC} + \overrightarrow{CD} + \overrightarrow{DE} + \overrightarrow{EF} + \overrightarrow{FA} = \overrightarrow{0}$ and $\overrightarrow{AB} + \overrightarrow{CD} + \overrightarrow{EF} = \overrightarrow{0}$, we must have $\overrightarrow{BC} + \overrightarrow{DE} + \overrightarrow{FA} = \overrightarrow{0}$. This means that those three vectors must form a closed polygon when put together head-to-tail, and since they are all equal in magnitude, this polygon is an equilateral triangle. Therefore the relative angles between them are 60 degrees, so if we extend the sides of the hexagon BC, DE, FA, they must form an equilateral triangle.

Problem 8. Let $S(n)$ be the maximum number of points we can have in n space where there are only two distinct pairwise distances between the points. (This means that for some real numbers d_1 and d_2, the distance between any given pair of points is either d_1 or d_2.) Show that

$$\lim_{n\to\infty} \frac{S(n)}{\frac{n^2}{2}} = 1.$$

Solution 8. We will prove that $S(n)$ can be lower bounded and upper bounded by quadratics with leading coefficient $\frac{1}{2}$.

Claim 1: $S(n) \geq \frac{n^2-n}{2}$.

Consider the set of points whose coordinates consist of two 1's and the rest 0's. We will show that this set satisfies the distance condition. Take any distinct P and Q in the set. If the coordinates that are 1 in P are at different locations than the coordinates that are 1 in Q, the distance between P and Q will be $\sqrt{(1-0)^2+(1-0)^2+(0-1)^2+(0-1)^2+(0-0)^2+(0-0)^2+\cdots} = 2$. If there is an overlap between one of the coordinates that is a 1 in P and Q, then we will have that the distance between P and Q is $\sqrt{(1-1)^2+(1-0)^2+(0-1)^2+(0-0)^2+(0-0)^2+\cdots} = \sqrt{2}$. Clearly both 1-coordinates cannot overlap or else P and Q would be the same point. Therefore we have found a set of points whose pairwise distances take on only two distinct values, and there are $\binom{n}{2}$ of these points (choosing two 1's from n possible coordinates). Therefore $S(n)$ must be at least $\binom{n}{2} = \frac{n^2-n}{2}$.

Claim 2: $S(n) \leq \frac{n^2+5n+6}{2}$.

Let $p_1, p_2, \cdots, p_m$ be a set of maximal size which satisfies the distance property (so $m = S(n)$), and let the coordinates of p_i be $a_{i,1}, a_{i,2}, \cdots, a_{i,n}$. Let the two possible pairwise distances be d_1 and d_2. For each point p_i we define the function f_i as follows:

$$f_i(x_1, x_2, \cdots, x_n) = \left(-d_1^2 + \sum_{j=0}^{n}(x_j - a_{i,j})^2\right)\left(-d_2^2 + \sum_{j=0}^{n}(x_j - a_{i,j})^2\right)$$

Looking at f_i, we see that for any point x, plugging in the coordinates $x_1, x_2, \cdots, x_n$ of x will give us the square distance between x and p_i minus the square of d_1, times the square distance between x and p_i minus the square of d_2. Therefore, for any p_j with $j \neq i$, we have f_i(coordinates of p_j) $= 0$ and f_i(coordinates of p_i) $\neq 0$.

We claim that $f_1, f_2, \cdots, f_m$ are linearly independent. To prove this, we assume for the sake of the contradiction that there exist constants $k_1, k_2, \cdots, k_m$, not all zero, such that $k_1 f_1 + k_2 f_2 + \cdots + k_m f_m = 0$. For each p_i, plugging the coordinates of p_i into $k_1 f_1 + k_2 f_2 + \cdots + k_m f_m$ removes all the terms except the ith since f_i(coordinates of p_j) $= 0$ for all $i \neq j$. This leaves only $k_i f_i$(coordinates of p_i) $= 0$ and since f_i(coordinates of p_i) $\neq 0$, we must have $k_i = 0$. This contradicts the assumption that the k_i were not all zero, so $f_1, f_2, \cdots, f_m$ are linearly independent.

Next, we define $f_{i,1}$ and $f_{i,2}$ as follows:

$$f_{i,1}(x_1, x_2, \cdots, x_n) = -d_1^2 + \sum_{j=0}^{n} (x_j - a_{i,j})^2$$
$$f_{i,2}(x_1, x_2, \cdots, x_n) = -d_2^2 + \sum_{j=0}^{n} (x_j - a_{i,j})^2$$

By definition, $f_i = (f_{i,1})(f_{i,2})$. We notice that $f_{1,1}, f_{1,2}, f_{2,1}, f_{2,2}, \cdots, f_{m,1}, f_{m,2}$ are all spanned by the vector space $\langle x_1^2 + x_2^2 + \cdots + x_n^2 \rangle, \langle x_1 \rangle, \langle x_2 \rangle, \cdots, \langle x_n \rangle, \langle 1 \rangle$. Meaning that, when expanded out, all of the functions $f_{1,1}, f_{1,2}, f_{2,1}, f_{2,2}, \cdots, f_{m,1}, f_{m,2}$ are of the form $k_1(x_1^2 + x_2^2 + \cdots + x_n^2) + k_2 x_1 + k_2 x_2 + \cdots k_{n+1} x_n + k_{n+2}(1)$ for some constants $k_1, k_2, \cdots, k_{n+2}$. (It is true that k_1 will always be 1, but that is irrelevant.)

Let $g(x_1, x_2, \cdots, x_n) = x_1^2 + x_2^2 + \cdots + x_n^2$. Since $f_i = (f_{i,1})(f_{i,2})$, and $f_{i,1}, f_{i,2}$ are spanned by $\langle g \rangle, \langle x_1 \rangle, \langle x_2 \rangle, \cdots, \langle x_n \rangle, \langle 1 \rangle$, we have that $f_1, f_2, \cdots, f_m$ are spanned by $\langle g^2 \rangle, \langle g * x_1 \rangle, \langle g * x_2 \rangle, \cdots, \langle g * x_n \rangle, \langle g * 1 \rangle, \langle x_1^2 \rangle, \langle x_1 * x_2 \rangle, \cdots, \langle x_1 * x_n \rangle, \langle x_1 * 1 \rangle, \langle x_2^2 \rangle, \cdots, \langle 1^2 \rangle$. Since the first vector space has dimension $n + 2$, this vector space has dimension $\binom{n+2}{2} + (n + 2) = \frac{n^2+5n+6}{2}$.

Now, consider the situation we have before us: there m linearly independent functions $f_1, f_2, \cdots, f_m$ which are spanned by a vector space with dimension $\frac{n^2+5n+6}{2}$. This implies that $m \leq \frac{n^2+5n+6}{2}$. Since $m = S(n)$, we are done.

Problem 9. (USA January TST 2015, Problem 3) Let ABC be a non-equilateral triangle and let M_a, M_b, M_c be the midpoints of the sides BC, CA, AB, respectively. Let S be a point lying on the Euler line. Denote by X, Y, Z the second intersections of M_aS, M_bS, M_cS with the nine-point circle. Prove that AX, BY, CZ are concurrent.

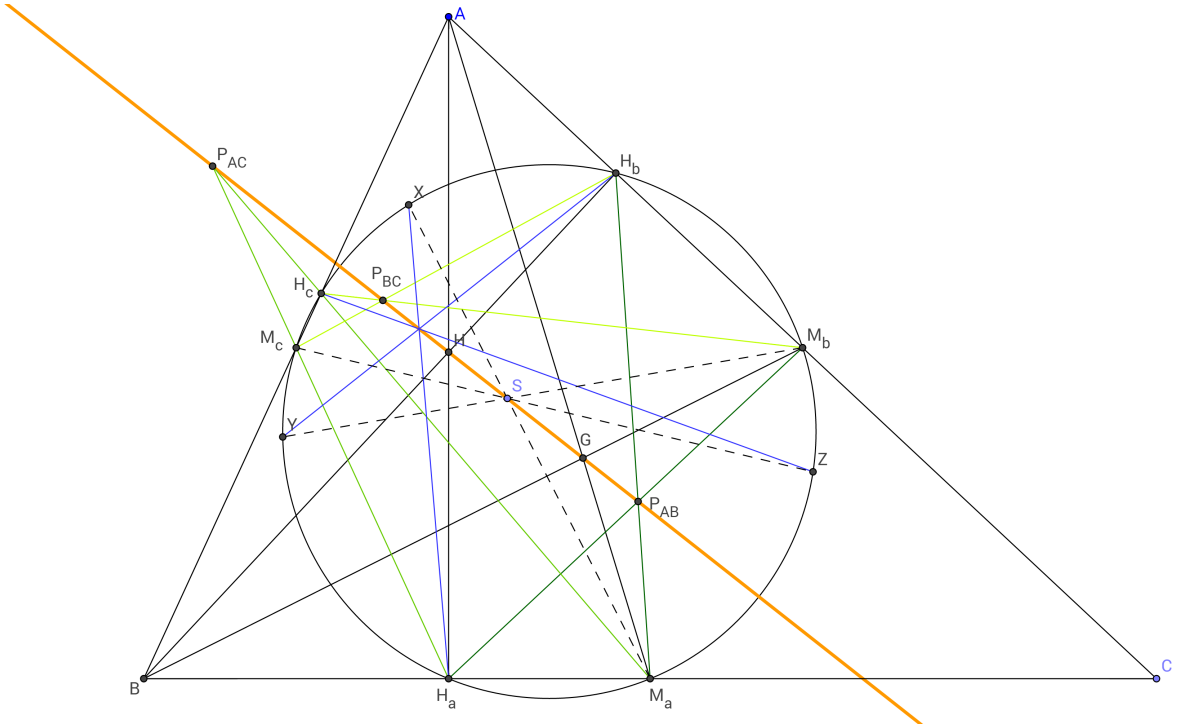

Solution 9. This problem is an illustrative example of how to angle chase in advanced Olympiad geometry. We combine the Law of Sines, cyclic quadrilaterals, and a creative lemma to solve this very difficult problem.

We first introduce the notation of the *cyclic product* of an expression. In the context of a symmetric triangle geometry problem, this represents the product of three quantities, each resembling the expression, but with the vertices A, B, C relabeled in a cyclic manner. For example, $\prod_{cyc} AB$ is $AB \cdot BC \cdot CA$, and $\prod_{cyc} \sin \angle XM_bC$ is $\sin \angle XM_bC \cdot \sin \angle YM_cA \cdot \sin \angle ZM_aB$ (since relabeling A also relabels M_a and X).

Let H_a, H_b, H_c be the feet of the altitudes of $\triangle ABC$, and let H and G be the orthocenter and centroid, respectively. It is well-known that the Euler line passes through G and H, and the nine-point circle passes through H_a, H_b, and H_c in addition to M_a, M_b, and M_c.

One of the main ways to prove that three lines concur is to use the trigonometric form of Ceva's Theorem, which, applied here, says that AX, BY, CZ concur if and only if

$$\prod_{cyc} \frac{\sin \angle XAB}{\sin \angle XAC} = 1.$$

There is not very much to be said about these angles; they are not part of any cyclic quadrilateral, nor are they easy to compute. Thus, we use the Law of Sines, on triangles XAM_c and XAM_b, to replace them:

$$\frac{\sin \angle XAB}{\sin \angle XAC} = \frac{\sin \angle XAM_c}{\sin \angle XAM_b} = \frac{\sin \angle XM_cA \cdot \frac{XM_c}{XA}}{\sin \angle XM_bA \cdot \frac{XM_b}{XA}} = \frac{\sin \angle XM_cA}{\sin \angle XM_bA} \cdot \frac{XM_c}{XM_b}.$$

We can easily analyze the second part of the product. Since it is a ratio of the sides of $\triangle XM_bM_c$, it is natural to use the Law of Sines. The resulting angles are part of a cyclic quadrilateral:

$$\frac{XM_c}{XM_b} = \frac{\sin \angle XM_bM_c}{\sin \angle XM_cM_b} = \frac{\sin \angle XM_aM_c}{\sin \angle XM_aM_b}.$$

Therefore,

$$\prod_{cyc} \frac{\sin \angle XAB}{\sin \angle XAC} = \prod_{cyc} \frac{\sin \angle XM_cA}{\sin \angle XM_bA} \cdot \prod_{cyc} \frac{XM_c}{XM_b} = \prod_{cyc} \frac{\sin \angle XM_cA}{\sin \angle XM_bA} \cdot \prod_{cyc} \frac{\sin \angle XM_aM_c}{\sin \angle XM_aM_b} = \prod_{cyc} \frac{\sin \angle XM_cA}{\sin \angle XM_bA},$$

where we have used that $\prod_{cyc} \frac{\sin \angle XM_aM_c}{\sin \angle XM_aM_b} = 1$ by Trigonometric Ceva on $\triangle M_aM_bM_c$ with cevians XM_a, YM_c, and ZM_c (which concur at S).

So we have reduced the problem to showing that $\prod_{cyc} \frac{\sin \angle XM_cA}{\sin \angle XM_bA} = 1$. It is not hard to see that $\angle XM_cA$ is either equal to or supplementary to $\angle XM_cH_c$ (which implies $\sin \angle XM_cA = \sin \angle XM_cH_c$), and since by definition X is on the the nine-point circle, $\angle XM_cH_c$ is either equal to or supplementary to $\angle XM_aH_c$, which we can write as $\angle SM_aH_c$. This eliminates from consideration the points X, Y, and Z:

$$\prod_{cyc} \frac{\sin \angle XM_cA}{\sin \angle XM_bA} = \prod_{cyc} \frac{\sin \angle XM_cH_c}{\sin \angle XM_bH_b} = \prod_{cyc} \frac{\sin \angle XM_aH_c}{\sin \angle XM_aH_b} = \prod_{cyc} \frac{\sin \angle SM_aH_c}{\sin \angle SM_aH_b}$$

We have not yet used the fact that S is on the Euler line. Thus, we introduce the following Lemma:

Key Lemma: Define P_{ab} to be the intersection of the lines H_aM_b and H_bM_a, and define P_{bc} and P_{ca} analogously. Then P_{ab}, P_{bc}, and P_{ca} lie on the Euler line.

Proof: We use Pappus's Theorem on the lines $\overline{AH_bM_b}$ and $\overline{BH_aM_a}$, which gives that G (the intersection of AM_a and BM_b), H (the intersection of AH_a and BH_b), and P_{ab} (the intersection of H_bM_a and H_aM_b) are collinear. This implies P_{ab} is on the Euler line, and by the same argument, so are P_{bc} and P_{ca}.

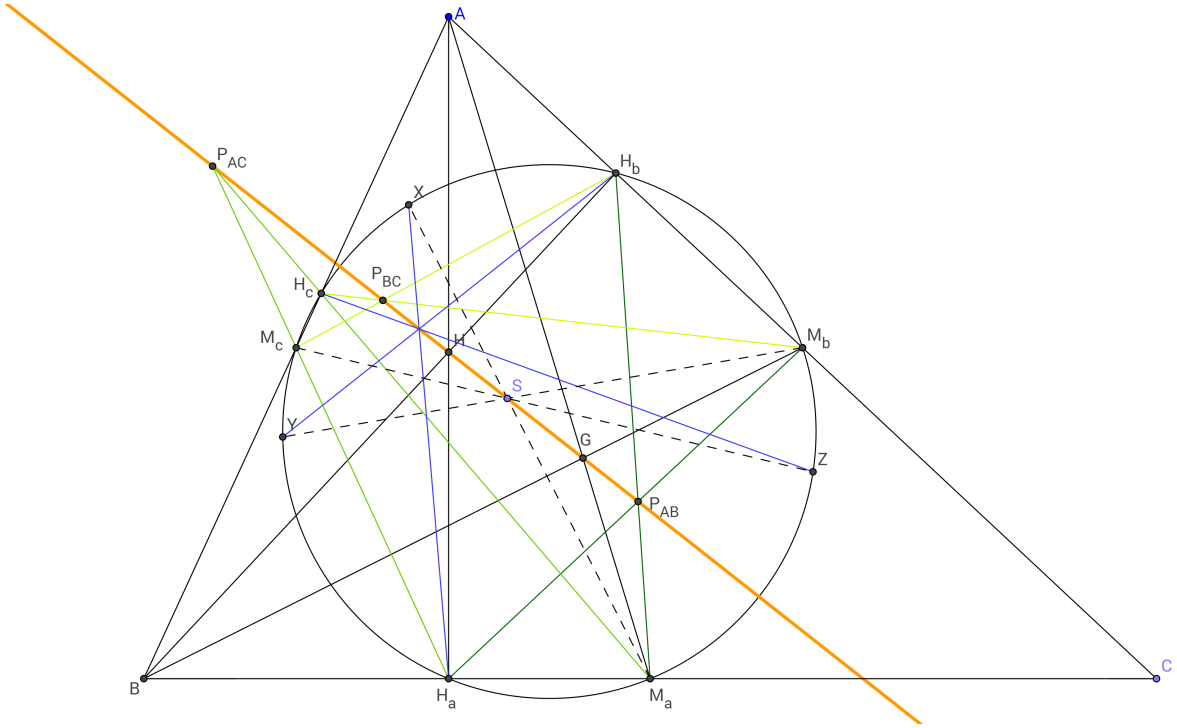

A corollary of the Lemma is that $\sin\angle P_{ca}SM_a = \sin\angle P_{ab}SM_a$. This gives us some cancellation after using the Law of Sines (again):

$$\prod_{cyc}\frac{\sin\angle SM_aH_c}{\sin\angle SM_aH_b} = \prod_{cyc}\frac{\sin\angle SM_aP_{ca}}{\sin\angle SM_aP_{ab}} = \prod_{cyc}\frac{\sin\angle P_{ca}SM_a\cdot\frac{SP_{ca}}{M_aP_{ca}}}{\sin\angle P_{ab}SM_a\cdot\frac{SP_{ab}}{M_aP_{ab}}} = \left(\prod_{cyc}\frac{SP_{ca}}{SP_{ab}}\right)\left(\prod_{cyc}\frac{M_aP_{ab}}{M_aP_{ca}}\right).$$

Since $\prod_{cyc}\frac{SP_{ca}}{SP_{ab}} = \frac{SP_{ca}}{SP_{ab}}\cdot\frac{SP_{ab}}{SP_{bc}}\cdot\frac{SP_{bc}}{SP_{ca}} = 1$, we now only need to show that $\prod_{cyc}\frac{M_aP_{ab}}{M_aP_{ca}} = 1$. Notice that we have eliminated S from the problem! The finish is a straightfoward calculation.

$$\prod_{cyc}\frac{M_aP_{ab}}{M_aP_{ca}} = \frac{M_aP_{ab}}{M_aP_{ca}}\cdot\frac{M_bP_{bc}}{M_bP_{ab}}\cdot\frac{M_cP_{ca}}{M_cP_{bc}} = \frac{M_aP_{ab}}{M_bP_{ab}}\cdot\frac{M_bP_{bc}}{M_cP_{bc}}\cdot\frac{M_cP_{ca}}{M_aP_{ca}} = \prod_{cyc}\frac{M_aP_{ab}}{M_bP_{ab}} = \prod_{cyc}\frac{\sin\angle M_aM_bP_{ab}}{\sin\angle M_bM_aP_{ab}}$$
$$= \prod_{cyc}\frac{\sin\angle M_aM_bH_a}{\sin\angle M_bM_aH_b} = \frac{\sin\angle M_aM_bH_a}{\sin\angle M_bM_aH_b}\cdot\frac{\sin\angle M_bM_cH_b}{\sin\angle M_cM_bH_c}\cdot\frac{\sin\angle M_cM_aH_c}{\sin\angle M_aM_cH_a} = 1.$$

The last equality follows because M_a, M_b, M_c, H_a, H_b, H_c lie on a circle, which gives $\sin\angle M_aM_bH_a = \sin\angle M_aM_cH_a$, $\sin\angle M_bM_aH_b = \sin\angle M_bM_cH_b$, and $\sin\angle M_cM_bH_c = \sin\angle M_cM_aH_c$. This completes the proof.

Alternate Proof: We also provide a proof which is shorter and perhaps more elegant, though more difficult to think of.

Recall that we reduced the problem to proving that $\prod_{cyc} \frac{\sin\angle XM_cA}{\sin\angle XM_bA} = 1$. In the original solution, we showed $\sin\angle XM_cA = \sin\angle SM_aH_c$ and thus eliminated X, Y, and Z from consideration. Instead, we can just as easily show that $\sin\angle XM_cA = \sin\angle XH_aH_c$. Then we need to prove that

$$\prod_{cyc} \frac{\sin\angle XH_aH_c}{\sin\angle XH_cH_a} = 1.$$

By the trigonometric form of Ceva's Theorem, with $\triangle H_aH_bH_c$ and cevians H_aX, H_bY, and H_cZ, this is equivalent to the concurrence of H_aX, H_bY, and H_cZ. Indeed, as we can see in the diagram, these three lines concur on the Euler line. To show this, we apply Pascal's Theorem to the cyclic hexagon $M_aXH_aM_bYH_b$ (in that order). This gives that H_aX and H_bY intersect on the line connecting S and P_{ab}, which, by the Key Lemma, is the Euler line. Similarly, H_aX and H_cZ intersect on the Euler line. Hence, H_aX, H_bY, and H_cZ concur on the Euler line, and we are done.

A beautiful generalization. Let P be a point inside $\triangle ABC$, and let Q be its isogonal conjugate. Let P_a, P_b, P_c be the feet of the altitudes from P to the sides BC, CA, AB, respectively. Similarly define Q_a, Q_b, Q_c. It is well-known that P_a, P_b, P_c, Q_a, Q_b, Q_c lie on a circle, which we call the six-point circle. (Prove this!) Let S be a point lying on line PQ. Denote by X, Y, Z the second intersections of P_aS, P_bS, P_cS with the six-point circle. Prove that AX, BY, CZ are concurrent, and also that Q_aX, Q_bY, Q_cZ, and PQ are concurrent. *The original problem is a special case of this result where we take P and Q to be O and H, respectively.*

Hint: Show that the center of the six-point circle is the midpoint of PQ, and then use Pascal's Theorem in the same style as the Alternate Solution.